



**NAVAL
POSTGRADUATE
SCHOOL**

MONTEREY, CALIFORNIA

THESIS

INTEGRATING THE FEL ON AN ALL-ELECTRIC SHIP

by

Charles A. Allen III

June 2007

Thesis Advisor:
Second Reader:

William B. Colson
Robert L. Armstead

Approved for public release; distribution is unlimited

THIS PAGE INTENTIONALLY LEFT BLANK

REPORT DOCUMENTATION PAGE			<i>Form Approved OMB No. 0704-0188</i>
Public reporting burden for this collection of information is estimated to average 1 hour per response, including the time for reviewing instruction, searching existing data sources, gathering and maintaining the data needed, and completing and reviewing the collection of information. Send comments regarding this burden estimate or any other aspect of this collection of information, including suggestions for reducing this burden, to Washington headquarters Services, Directorate for Information Operations and Reports, 1215 Jefferson Davis Highway, Suite 1204, Arlington, VA 22202-4302, and to the Office of Management and Budget, Paperwork Reduction Project (0704-0188) Washington DC 20503.			
1. AGENCY USE ONLY (Leave blank)	2. REPORT DATE June 2007	3. REPORT TYPE AND DATES COVERED Master's Thesis	
4. TITLE AND SUBTITLE Integrating the FEL on an All-Electric Ship		5. FUNDING NUMBERS	
6. AUTHOR(S) Charles A. Allen III		8. PERFORMING ORGANIZATION REPORT NUMBER	
7. PERFORMING ORGANIZATION NAME(S) AND ADDRESS(ES) Naval Postgraduate School Monterey, CA 93943-5000		10. SPONSORING/MONITORING AGENCY REPORT NUMBER	
9. SPONSORING /MONITORING AGENCY NAME(S) AND ADDRESS(ES) N/A		11. SUPPLEMENTARY NOTES The views expressed in this thesis are those of the author and do not reflect the official policy or position of the Department of Defense or the U.S. Government.	
12a. DISTRIBUTION / AVAILABILITY STATEMENT Approved for public release; distribution is unlimited.		12b. DISTRIBUTION CODE	
13. ABSTRACT (maximum 200 words) <p>This thesis examines the feasibility of placing the free electron laser (FEL) on the all-electric ship. The power required by the FEL and the tolerance of the FEL to vibrations is determined using computer simulations. Methods of reducing the vibrations using vibration isolation and active alignment are described. The simulations show that the all-electric ship will provide more than enough power to operate the FEL. The results also indicate that there must be methods to reduce the effect of ship vibrations in order for the FEL to reach the desired output power of one to three megawatts.</p> <p>The thesis also describes the physical dimensions of the FEL as well as its weight and cost, and compares these figures to other ship systems. Overall the simulations and the research show that it is reasonable that a high-powered FEL can be developed for use as a weapon on the all-electric ship. While developing such a weapon will be an engineering challenge the capability to do so has been demonstrated.</p>			
14. SUBJECT TERMS Free Electron Laser, FEL, All-Electric Ship, Directed Energy, Vibration Mitigation		15. NUMBER OF PAGES 75	
		16. PRICE CODE	
17. SECURITY CLASSIFICATION OF REPORT Unclassified	18. SECURITY CLASSIFICATION OF THIS PAGE Unclassified	19. SECURITY CLASSIFICATION OF ABSTRACT Unclassified	20. LIMITATION OF ABSTRACT UL

THIS PAGE INTENTIONALLY LEFT BLANK

Approved for public release; distribution is unlimited

INTEGRATING THE FEL ON AN ALL-ELECTRIC SHIP

Charles A. Allen III
Ensign, United States Navy
B.S., Embry-Riddle Aeronautical University, 2006

Submitted in partial fulfillment of the
requirements for the degree of

MASTER OF SCIENCE IN APPLIED PHYSICS

from the

NAVAL POSTGRADUATE SCHOOL
June 2007

Author: Charles A. Allen III

Approved by: William B. Colson
Thesis Advisor

Robert L. Armstead
Second Reader

James H. Luscombe
Chairman, Department of Physics

THIS PAGE INTENTIONALLY LEFT BLANK

ABSTRACT

This thesis examines the feasibility of placing the free electron laser (FEL) on the all-electric ship. The power required by the FEL and the tolerance of the FEL to vibrations is determined using computer simulations. Methods of reducing the vibrations using vibration isolation and active alignment are described. The simulations show that the all-electric ship will provide more than enough power to operate the FEL. The results also indicate that there must be methods to reduce the effect of ship vibrations in order for the FEL to reach the desired output power of one to three megawatts.

The thesis also describes the physical dimensions of the FEL as well as its weight and compares these figures to other ship systems. Overall the simulations and the research show that it is reasonable that a high-powered FEL can be developed for use as a weapon on the all-electric ship. While developing such a weapon will be an engineering challenge the capability to do so has been demonstrated.

THIS PAGE INTENTIONALLY LEFT BLANK

TABLE OF CONTENTS

I.	INTRODUCTION.....	1
II.	DESCRIPTION OF FEL COMPONENTS AND THEORY.....	3
A.	FEL COMPONENTS.....	3
1.	Photoinjector.....	3
2.	Superconducting Linear Accelerator.....	5
3.	Undulator.....	6
4.	Optical Cavity (Oscillator Configuration).....	8
5.	Optics (Amplifier Configuration).....	9
6.	Recirculation and Beam Dump.....	9
B.	FEL PHYSICS.....	10
1.	Undulator Fields and the Resonance Condition.....	10
2.	Pendulum Equation and Electron Motion.....	12
3.	The Wave Equation.....	14
4.	FEL Gain and Phase Space Plots.....	15
III.	ENERGY REQUIREMENTS.....	19
A.	ESTIMATED POWER REQUIREMENT.....	19
B.	EFFICIENCY OF THE FEL.....	21
1.	Klystron and IOT Descriptions.....	21
2.	FEL Efficiency Calculation.....	24
C.	POWER GENERATION.....	26
IV.	SHIP MOTION AND FEL TOLERANCE.....	27
A.	SHIP MOTION.....	27
B.	FEL TOLERANCE.....	29
1.	FEL Designs.....	29
2.	Electron Beam Shift.....	35
3.	Electron Beam Tilt.....	36
4.	Mirror Shift.....	37
5.	Mirror Tilt.....	38
V.	VIBRATION DAMPING.....	41
A.	VIBRATION ISOLATION.....	41
B.	ACTIVE ALIGNMENT.....	44
VI.	WEIGHT, COST, AND SIZE.....	47
A.	FEL WEIGHT AND SIZE.....	47
B.	FEL COST.....	49
VII.	CONCLUSION.....	51
	LIST OF REFERENCES.....	53
	INITIAL DISTRIBUTION LIST.....	55

THIS PAGE INTENTIONALLY LEFT BLANK

LIST OF FIGURES

Figure 1.	Diagram of a photoinjector [From 2].	4
Figure 2.	Accelerator cavity of a superconducting linear accelerator.	5
Figure 3.	Diagram of undulator including the optical beam [From 4].	7
Figure 4.	Electron in resonance with optical beam [From 6, a].	12
Figure 5.	Phase space plot of electron evolution [From 6,a].	17
Figure 6.	3MW FEL with power requirements for each system [From 7].	20
Figure 7.	Two cavity klystron [From 9].	22
Figure 8.	Multicavity klystron [From 11].	23
Figure 9.	IOT cross section [From 12].	24
Figure 10.	One-megawatt oscillator FEL design at 1.6micron wavelength.	35
Figure 11.	Extraction versus electron beam shift for 100kW FEL amplifier design.	36
Figure 12.	Optical energy in an oscillator FEL with an electron beam tilt.	37
Figure 13.	Optical energy in an oscillator FEL with a mirror shift.	38
Figure 14.	Extraction versus mirror shift in Jefferson Lab FEL.	38
Figure 15.	Optical energy in an oscillator FEL with a mirror tilt.	39
Figure 16.	Diagram of a mass-spring-dashpot system with a vibrating support structure [From 13].	41
Figure 17.	Transmissibility as a function of frequency ratio [From 13].	43
Figure 18.	Diagram of mirror placement in LSST [From 14].	45
Figure 19.	Graph of the cost, efficiency, weight, RF cost and size of 100kW, 1MW and 3MW FEL designs [From 7].	49

THIS PAGE INTENTIONALLY LEFT BLANK

LIST OF TABLES

Table 1.	FFG-7 ship motions maximum amplitude minimum period.	28
Table 2.	MIL-STD-167-1A vibration displacement criteria for variable frequency test.....	28
Table 3.	Electron beam properties for oscillator FEL designs.....	30
Table 4.	Electron beam properties for amplifier FEL designs.....	31
Table 5.	Undulator properties for oscillator FEL designs.....	31
Table 6.	Undulator properties for amplifier FEL designs.....	32
Table 7.	Optical cavity specifications for oscillator FEL designs.....	33
Table 8.	Optical specifications for amplifier FEL designs.....	34
Table 9.	Power outputs of high power FEL designs.....	35
Table 10.	Tolerances for mirror and camera alignment of LSST.....	44
Table 11.	Weight of FEL components of one and three-megawatt designs.....	47

THIS PAGE INTENTIONALLY LEFT BLANK

LIST OF ACRONYMS

AES	Advanced Energy Systems
cm	Centimeter
DC	Direct Current
FEL	Free Electron Laser
FWHM	Full width half maximum
Hz	Hertz
IOT	Inductive Output Tube
IR	Infrared
K	Kelvin
kg	Kilogram
kW	Kilo-Watts
LSST	Large Synoptic Survey Telescope
m	Meter
MeV	Mega-Electron Volt
MHz	Mega-Hertz
mm	Millimeter
MW	Mega-Watt
RF	Radio Frequency
SLAC	Stanford Linear Accelerator
SLINAC	Superconducting Linear Accelerator
SRF	Superconducting Radio Frequency
UHF	Ultra High Frequency
W	Watts

THIS PAGE INTENTIONALLY LEFT BLANK

LIST OF SYMBOLS

a	Optical field amplitude
\vec{A}	Vector field potential
\vec{B}	Magnetic field
B	Magnetic field magnitude
\vec{B}_o	Magnetic field of optical field
\vec{B}_U	Magnetic field of the undulator
c	Speed of light
c	Damping coefficient
c_{char}	Characteristic damping coefficient
c_{crit}	Critical damping coefficient
e	Magnitude of electron charge
\vec{E}	Electric field
E	Magnitude of electric field
G	Optical field gain
I	Electron beam current
j	Dimensionless current density
\vec{J}_\perp	Transverse current density
K	Undulator parameter
k	Spring constant
k	Optical wave number
k_o	Undulator wave number

L	Undulator length
m	Electron mass
m	Mass in spring-and-damper isolator
N	Number of periods
P	Optical power
P_{in}	Power input into the FEL
P_o	Fixed power
P_{cryo}	Power required for cryoplant
P_{aux}	Power required for auxiliary systems
Q	Quality factor of damper
Q_n	Quality factor of mirror
r	Frequency ratio
T	Transmissibility
V_{inj}	Injector voltage
$\langle V' \rangle$	Average beam dump voltage
x_m	Mass motion
x_s	Structure motion
z	Undulator direction
$\bar{\beta}$	Non dimensional electron velocity
β_{\perp}	Magnitude of transverse non-dimensional electron velocity
ϕ	Initial optical phase
γ	Lorentz factor
η	FEL extraction

η_{RF}	Klystron/IOT efficiency
η_{WP}	Wall-plug efficiency
λ	Optical wavelength
λ_o	Undulator wavelength
ν	Electron phase velocity
ρ_e	Electron density
ζ	Damping ratio
τ	Dimensionless time
ω	Optical frequency
ω	Vibration frequency
ω_0	Resonant frequency
ψ	Optical phase
ζ	Electron phase

THIS PAGE INTENTIONALLY LEFT BLANK

I. INTRODUCTION

The free electron laser (FEL) uses a beam of electrons to generate and amplify an optical beam. The purpose of the FEL as a weapon on a ship will be to defend the ship against anti-ship missiles as well as small vessels and aircraft. It may also be used to destroy enemy communications or to disable enemy satellites. The benefits of the FEL over other weapons and other types of lasers are that the FEL has a designable wavelength, is efficient, and has a deep magazine. Since the FEL has a designable wavelength (tunable in fact), it can be built and adjusted so that the laser beam propagates through the atmosphere with minimal losses. It is also efficient when compared to other types of lasers, and this reduces the power requirements. The FEL also has a nearly unlimited magazine since it only requires electrical power.

The purpose of this thesis is to examine the feasibility of placing the FEL onto the all-electric ship. The components and physics of the FEL are explained, the power requirements are examined, and it is determined that the all-electric ship will have sufficient power to operate the FEL. Ship vibrations and the tolerance of the FEL to displacements are shown using simulations. Methods to reduce vibration are examined and it is shown that similar methods have been used in the airborne laser program. Also the weight, size and cost of the FEL are outlined.

The information gathered and the simulations, show that it should be possible to integrate the FEL into the all-electric ship. The physics is clear, and the engineering challenges are surmountable.

THIS PAGE INTENTIONALLY LEFT BLANK

II. DESCRIPTION OF FEL COMPONENTS AND THEORY

The FEL operates on the principle that an electron bunch will radiate coherently when accelerated in a direction transverse to its forward velocity by the static magnetic field of the undulator. This magnetic field oscillates in space with a period of a few centimeters. The FEL uses a high energy electron beam traveling through the undulator to produce the optical energy. The electrons are moving at relativistic speeds with a Lorentz Factor much greater than one, and we will see that for relativistic electrons the wavelength of the laser light is much smaller than the undulator period.

A. FEL COMPONENTS

The components of the FEL, first generate the required electron beam and then guide this beam to the undulator, where the electron beam radiates optical energy. The components required to generate and control the electron and optical beams will be examined in the following sections, while auxiliary systems such as power and refrigeration will be covered in later sections. The electron beam is enclosed in a vacuum while the optical beam interacts with electrons in a vacuum, and then is transported through a transparent window to the air.

1. Photoinjector

The photoinjector is the source of the electrons making up the electron beam. The photoinjector must produce bunches of electrons at the frequency that matches a multiple of the accelerator frequency, and must also produce these bunches with small emittance. Emittance describes the collimation of the electron beam. For the FEL weapon design the bunches will also need to be short during the interaction, about 1ps long, and have a charge of about 1nC, so that the peak current is large, around 1kA, and the average current is about 1A.

The photoinjector considered here consists of two main components: the DC gun and a superconducting radio frequency (SRF) injector. The DC gun creates the electron bunches, which flow into the SRF injector to be accelerated to the energy required for the accelerator section of the FEL.

In the DC gun, a pulsed laser is focused on a photocathode, which is in a strong DC electric field. The laser considered here operates at the same frequency as the accelerator, about 700MHz, and when the photons of the laser strike the photocathode, electrons escape from the material and are carried away by the electric field. The photocathode itself is a metal such as Gallium Arsenide (Jefferson Lab), Cs₂Te, CsK₂Sb, or Cu [1]. A diagram of a DC photoinjector is shown in Figure 1. The laser is shown locked at the same frequency as the RF drive, and when the laser strikes the photoemitter it will give off electrons. The DC voltage required to get the desired bunch characteristics is a few hundred kilovolts. At this point the electron beam is not at the required energy to enter the superconducting linear accelerator (SLINAC) so it must be accelerated and also bunched more tightly by the SRF injector.

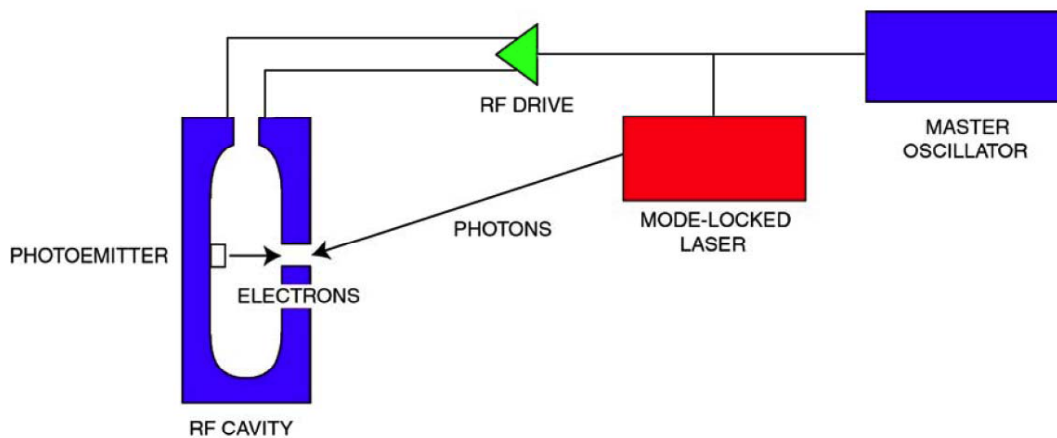


Figure 1. Diagram of a photoinjector [From 2].

The SRF injector operates at the same frequency of about 700MHz as the SLINAC and accelerates the electron bunches to an energy of about 5MeV. The SRF injector consists of two superconducting cells, each raising the energy by about 2MeV, which are being fed RF power and resonate at about 700MHz [3]. As the electrons enter

the first cell they are accelerated, and the electrons which reach the second cell before the field changes will not be accelerated as much. In this way, the electrons are bunched more closely and also accelerated to the energy required by the SLINAC.

2. Superconducting Linear Accelerator

In the FEL weapon design, the electron beam must be at an energy of about 80MeV by the time it reaches the undulator in order to produce an optical energy of 1MW at the desired wavelength of about one micron. The electron beam will pass through the SLINAC after exiting the SRF injector and will be accelerated in much the same way as in the SRF injector.

The SLINAC consists of many cells of a superconducting material such as niobium cooled to 2K. These cells are ellipsoidal with a passage through the center for the electron beam to travel through, as shown in Figure 2. The accelerator is divided into cavities each about a meter in length. The cavities are arranged end to end until the required length of accelerator is in place to meet the desired electron beam energy. The accelerator raises the electron beam energy at a gradient of about 10MeV/m. So about 8-10m of accelerator is required to produce 80-100MeV for the 1MW FEL.



Figure 2. Accelerator cavity of a superconducting linear accelerator.

The accelerator works on the principle that the electron bunch coming from the injector will be accelerated in the presence of a positive electric field. When RF power is fed into the SLINAC, the accelerator is designed to resonate at the same frequency as the RF power at 700MHz. Because of the high frequency of the RF power, the accelerator

must be superconducting to keep the losses due to electrical resistance low. The electric field established in each cell from the RF power will oscillate between positive and negative, thus attracting and repulsing the electrons in the electron bunch. The frequency of the accelerator is synchronized with the injector so that when the electron bunch reaches the entrance of the accelerator, the first cell will have a positive electric field accelerating the electron bunch to the next cell. This will occur for each cell until the electrons reach the desired energy of 80-100MeV at the exit of the accelerator.

Besides accelerating the electrons up to higher velocities, the accelerator also performs an important role in compacting the bunch length. The electron bunch is an extended charge, and some electrons entering the SLINAC have a higher velocity than the rest of the bunch. When the electron bunch enters the first cell and is accelerated, the faster electrons will reach the next cell first, when it has a smaller accelerating electric field, so the faster electrons will slow with respect to the rest of the bunch. By the time the rest of the bunch reaches the next cell its electric field will have changed to accelerate the electrons. Since this process occurs throughout the SLINAC, the electron beam bunch length is reduced.

The SLINAC prepares the electron beam for the undulator by bringing the electrons to an energy where they will produce about one micron radiation and by bunching the electron pulse tighter. The SLINAC is a relatively large component of the FEL in terms of size, being about 10m long. It also uses most of the RF power and must be refrigerated to 2K.

3. Undulator

The undulator is where energy of the electron beam is transferred into optical energy, and is of central importance in determining the characteristics of the optical beam of the FEL. An FEL is either an amplifier or an oscillator. In the amplifier configuration, the undulator is, typically about 2m to 10m long, and a seed laser provides an initial optical field entering the undulator. This light is then amplified by the interaction with the electron beam in the undulator. In the oscillator or resonator configuration, the electron beam emits light when traveling through a shorter undulator of about 0.5-2m in

length. As the optical energy bounces between the mirrors, it is amplified through each pass of the undulator. Both configurations are being examined for weapons use.

The undulator consists of permanent magnets or electromagnets to produce a magnetic field transverse to the electron beam axis. Figure 3 shows how the electron beam traveling through the undulator will accelerate in a transverse direction and radiate. The magnets are spaced in this FEL about 3cm apart. There are about 20 periods in the oscillator configuration meaning that the magnetic field changes direction 40 times through the undulator. In the amplifier configuration, the undulator has about 100 to 200 periods. When the electron beam passes through these changing magnetic fields, the electrons will bunch in each optical wavelength and many will lose kinetic energy, emitting and amplifying the optical field. The physics will be examined in more detail in the theory section.

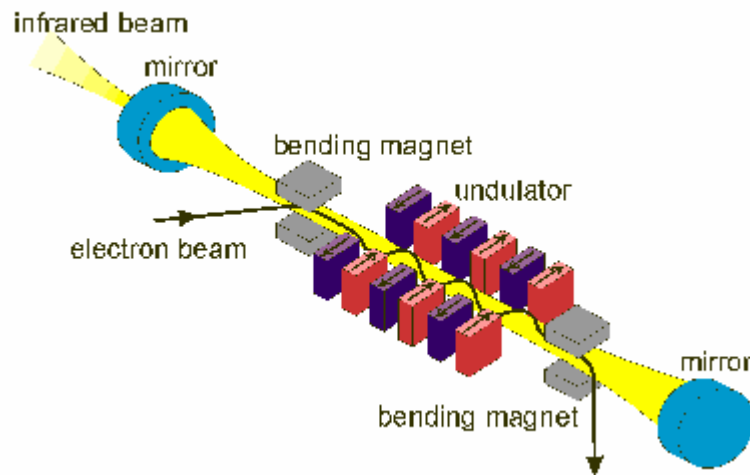


Figure 3. Diagram of undulator including the optical beam [From 4].

The amplifier configuration requires that the undulator be tapered in order to produce enough extraction to reach the desired energy of about 1MW. “Tapering” is a change in the strength of the magnetic field along the length of the undulator. This is usually done by physically moving the magnets further from the electron beam or, if using electromagnets, by reducing the magnets’ strength. The tapering usually causes the magnetic field to decrease from the entrance of the undulator to the exit.

4. Optical Cavity (Oscillator Configuration)

The optical cavity of an oscillator FEL consists of two mirrors aligned so that the light will be focused at the undulator. The optical cavity is where the light produced from the undulator is stored by bouncing in between the mirrors as seen in Figure 3.

The mirrors are typically spaced about 20m apart, have about a 5 to 10cm radius each, and are specifically designed to work at the wavelength of one micron. However the intensity can be so great (about $200\text{kW}/\text{cm}^2$), that they must be cooled by a cryogenic liquid so that they do not discolor, damage or distort to the degree that the laser fails to operate.

The intensity on the mirrors is kept relatively low despite the high intensity in the oscillator, due to the fact that the radius of curvature of the mirrors is chosen so that there is a short Rayleigh length. This means that the optical energy is tightly focused at the center of the undulator to a radius of about 0.1mm and rapidly expands out to the mirrors with a radius of about 3cm. Without this rapid expansion the optical beam radius at the mirrors would be much smaller and the intensity on the mirrors would be too great.

The mirrors are separated by a distance so that the sequence of electron pulses enters the undulator with an optical pulse slightly behind it. This is called “synchronism” and it is necessary so that the optical pulse and electron pulse travel through the undulator together.

One mirror in the oscillator is totally reflective while the other is partially transmissive, which in the FEL weapons system will have a quality factor of about $Q_n=2$, meaning half of the light that strikes it will be transmitted through it. This allows the optical energy to leave the oscillator and enter the optical beam path where it will be directed to the beam director and finally to the target. The quality factor of the mirror is chosen so that the optimum energy can be released, in this case a megawatt, but at the same time have enough optical energy stored in the oscillator so that the laser will have enough gain at low power to reach steady state. In other words, if too much optical energy leaks out when the laser is starting it will never be able to amplify the light at the rate that light is leaking out.

5. Optics (Amplifier Configuration)

In the amplifier configuration, the optical path is different than in the oscillator configuration. The optical path is in a vacuum and contains a seed laser, which fires optical pulses through the undulator, and these pulses are amplified by the electron pulses. After exiting the undulator, the optical energy then strikes the first reflective mirror of the beam path to the beam director and out to the target.

The seed laser is timed at the same frequency as the injector and accelerator at 700MHz so that the optical pulses it fires are at the same frequency as the electron pulses entering the undulator. The optical pulses are timed so that they will enter the undulator at the same time that an electron pulse is entering.

The seed laser is a solid state laser which will produce light at the wavelength of about one micron and it is estimated to have an average energy of about 100W. This optical seed pulse is amplified through the interaction with the electrons in the undulator to produce average output energy of about 1MW.

Since the amplifier must rely on diffraction to spread the optical beam, the first mirror is about 10m from the undulator and is at a shallow angle so that the light glances off of it and it does not overheat and become damaged. This first mirror will spread the optical beam so that it can be transmitted to the beam director without the intensity on the mirrors causing any damage. Since the first mirror is reflective, it can be cooled from the back surface.

6. Recirculation and Beam Dump

After the electron beam has passed through the undulator and amplified the optical beam, it has lost a few percent of its energy. The electron beam still has most of its energy, and instead of wasting this energy, it is used to regenerate the RF power of the SLINAC.

The electrons exiting the undulator must be bent by magnets to return back to the accelerator. To ensure that the electrons are properly bent they are required to have an energy spread of less than about 15% when leaving the undulator. Otherwise, the large

velocity spread would cause the electrons to turn at different rates in the same magnetic field and spread out too much to be sent through the SLINAC.

After going through the bending magnets, the electron beam will reenter the SLINAC out of phase with the electrons being accelerated. This will decelerate the electron beam and thus supply the SLINAC with RF power. When the electron beam exits the SLINAC, it will have an energy of about 5MeV. The deceleration process is another reason the induced energy spread cannot be too large. If too much energy is extracted from some electrons, they may reach zero energy before reaching the end of the deceleration process, and not make it to the beam dump.

After deceleration, the electron beam is then sent to the beam dump where the rest of the beam energy is dissipated; it is where the final kinetic energy of the electrons is absorbed by a piece of metal. The beam dump heats up when the FEL is operating and must be cooled. On a ship the beam dump will be cooled by seawater.

B. FEL PHYSICS

After examining the components of the FEL, the physics behind the generation of the optical field is described. The interaction between the electrons and the light will be examined and the creation of the optical energy will be shown.

1. Undulator Fields and the Resonance Condition

As the electrons pass through the undulator, their motion will be determined by the magnetic fields present from the undulator, as well as the electric and magnetic fields in the optical beam co-propogating through the undulator. Since the electrons are moving at relativistic velocities, their motion in the presence of these fields is determined by the relativistic Lorentz force equation [5],

$$\frac{d(\gamma\vec{\beta})}{dt} = -\frac{e}{mc}(\vec{E} + \vec{\beta} \times \vec{B}), \quad (2.1)$$

$$\gamma = \frac{1}{\sqrt{1-\beta^2}}, \quad (2.2)$$

$$\frac{d\gamma}{dt} = -\frac{e}{mc} \vec{\beta} \cdot \vec{E}, \quad (2.3)$$

$$\vec{\beta} = \frac{\vec{v}_e}{c}, \quad (2.4)$$

where γ is the relativistic Lorentz factor and is determined by equation 2.2, $\vec{\beta}$ is the ratio of the electron velocity to the speed of light in equation 2.4, e is the charge magnitude of an electron, m is the mass of an electron, c is the speed of light, \vec{E} is the total electric field present in the undulator, and \vec{B} is the total magnetic field in the undulator. Since the electron beam has an energy of about 80MeV when it enters the undulator, the Lorentz factor has a value of about $\gamma \approx 150$ and $\beta \approx 1$. Using the Lorentz force equation 2.1, the interaction between the static magnetic field produced by a helical undulator, and the magnetic and electric fields of the optical energy can be examined. The fields are given below

$$\vec{B}_U = B(\cos(k_0 z), \sin(k_0 z), 0) \quad (2.5)$$

$$\vec{E}_O = E(\cos \psi, -\sin \psi, 0) \quad (2.6)$$

$$\vec{B}_O = E(\sin \psi, \cos \psi, 0) \quad (2.7)$$

where the components in the z direction are all zero since the magnetic field from the undulator is transverse to the electron beam and the optical pulses travel in the z direction. The magnitude of the undulator magnetic field is B , k_0 is the wave number of the undulator and is related to the wavelength of the undulator by $\lambda_0 = 2\pi / k_0$. The magnitude of the electric field of the optical pulse is E , and $\psi = kz - \omega t + \phi$ where $k = 2\pi / \lambda$ is the optical wave number, z is the distance along the undulator axis, ω is the optical frequency, ϕ is the phase, and λ is the wavelength of the optical pulse.

The electrons will be accelerated in a direction transverse to their forward motion by the magnetic and electric fields described above. In order for the electrons to amplify the optical energy, they must interact with the optical and undulator fields shown above

in what is called the “resonance condition”. The resonance condition occurs when the electron z velocity is adjusted so that for every oscillation of the electron through the one period of the undulator, λ_0 , one wavelength of light will pass over the electron. The resonance condition is illustrated in Figure 4 where the electron in red is passed by one optical wavelength in blue, while traveling through one undulator wavelength.

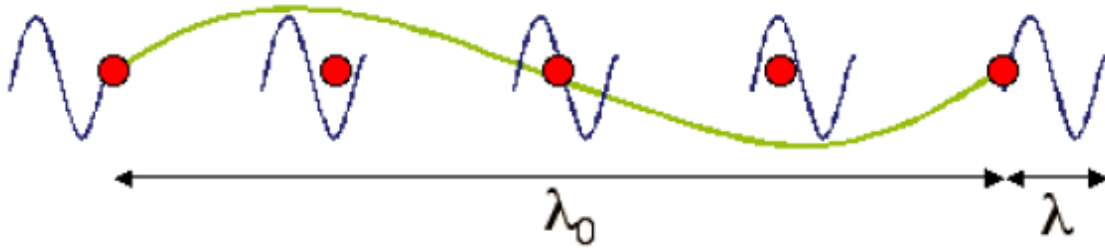


Figure 4. Electron in resonance with optical beam [From 6a].

The resonance condition exists when the electrons will travel a distance of λ_0 while the light wave will travel $\lambda + \lambda_0$. This is due to the fact that the electron beam is traveling at a velocity which is slightly less than the speed of light. The wavelength of the light emitted by the FEL is given by the following equation [6, b]:

$$\lambda \approx \frac{\lambda_0(1+K^2)}{2\gamma^2}, \text{ where} \quad (2.8)$$

$$K = \frac{eB\lambda_0}{2\pi mc^2}, \quad (2.9)$$

where K is called the undulator parameter, typically $K \approx 1$, and is a characteristic of the undulator design. From equation 2.8 it is clear that the wavelength of light produced by the FEL can be changed by varying the electron beam energy (represented by the Lorentz factor), the undulator period, or the field strength of the magnetic field of the undulator. This tunability of the optical wavelength is a benefit peculiar of the FEL.

2. Pendulum Equation and Electron Motion

The electron motion through the undulator is based on the optical and undulator fields shown in equations 2.5 through 2.7, and the force on the electrons is given by the

Lorentz force equation 2.1. If we put the fields inside the undulator (equations 2.5, 2.6, 2.7) into equation 2.1 we see that the transverse motion of the electrons is given by:

$$\frac{d(\gamma\beta_x)}{dt} = -\frac{e}{mc} [E(1-\beta_z)\cos\psi - \beta_z B \sin(k_0 z)], \text{ and} \quad (2.10)$$

$$\frac{d(\gamma\beta_y)}{dt} = -\frac{e}{mc} [-E(1-\beta_z)\sin\psi + \beta_z B \cos(k_0 z)], \quad (2.11)$$

where $\beta_z \approx 1$ since the electrons are traveling near the speed of light. This means that the value of $(1-\beta_z)$ is very small when compared to β_z and can be ignored. After integrating equations 2.10 and 2.11 and taking the constants of integration to be zero, meaning that there is perfect injection into the undulator, the transverse velocity is

$$\vec{\beta}_\perp = -\frac{K}{\gamma} (\cos(k_0 z), \sin(k_0 z), 0). \quad (2.12)$$

The rate of change of the electrons energy can be found by substituting the transverse velocity of equation 2.12 into equation 2.3. This results in the following:

$$\frac{d\gamma}{dt} = -\frac{e}{mc} E [\beta_x \cos\psi - \beta_y \sin\psi] = \frac{eKE}{\gamma mc} \cos(\zeta + \phi), \quad (2.13)$$

where $\zeta = (k + k_0)z - \omega t$ is the electron phase and can be thought of as the position of an electron within an optical wavelength. The change in electron energy can be related to the change in electron phase by

$$\frac{d\gamma}{dt} = \left(\frac{\gamma}{2k_0 c} \right) \frac{d^2\zeta}{dt^2}. \quad (2.14)$$

This can be solved for the rate of change of phase velocity by putting in equation 2.13 into equation 2.14, so that

$$\frac{d^2\zeta}{dt^2} = 2k_0 \frac{eKE}{\gamma^2 m} \cos(\zeta + \phi). \quad (2.15)$$

To more easily understand the meaning of this equation of motion, dimensionless time is defined as $\tau = ct/L$, where through the undulator τ varies from 0 to 1, and L is

the length of the undulator. Taking the derivative of the electron phase with respect to the dimensionless time gives the phase velocity

$$\dot{\nu} = \dot{\zeta} = L[(k + k_0)\beta_z - k], \quad (2.16)$$

where $(\dot{}) = d()/d\tau$ is the derivative with respect to dimensionless time. The electron equation of motion (2.15) then becomes the pendulum equation

$$\dot{\nu} = \dot{\zeta} = |a| \cos(\zeta + \phi) \quad (2.17)$$

where $|a| = \frac{4\pi NeKLE}{\gamma^2 mc^2}$ is the dimensionless field amplitude of the optical beam, and where N is the number of periods in the undulator. Equation 2.17 is the basis of the simulations, which analyze the progression of electrons in phase space.

3. The Wave Equation

After examining the interaction of the electron beam with the fields in the undulator, the evolution of the optical beam will be examined. The propagation of light is described by the wave equation

$$\left(\bar{\nabla}^2 - \frac{1}{c^2} \frac{\partial^2}{\partial t^2} \right) \vec{A} = -\frac{4\pi}{c} \vec{J}_\perp, \quad (2.18)$$

where $\vec{A} = (E/k)[\cos\psi, -\sin\psi, 0]$ is the vector field potential and \vec{J}_\perp is the current density transverse to the forward motion of the electrons due to the oscillations in the undulator. By substituting the complex vector potential into equation 2.18 and assuming that both the phase and field amplitude vary slowly, we derive that the field evolves according to

$$\frac{\partial}{\partial t}(Ee^{i\phi}) = -\frac{2\pi K e c \rho_e}{\gamma} \langle e^{-i\zeta} \rangle, \quad (2.19)$$

where ρ_e is the electron density and $\langle \dots \rangle$ is the average of all electrons. Using the dimensionless laser field a defined below equation 2.17 and the dimensionless time τ , the wave equation can be written as

$$\ddot{a} = -j \langle e^{-i\zeta} \rangle \quad (2.20)$$

where the dimensionless current density j is given by

$$j = \frac{8\pi^2 N e^2 K^2 L^2 \rho_e}{\gamma^3 m c^2}. \quad (2.21)$$

The dimensionless current density j represents the amount of coupling between the electron and laser beams. When the dimensionless current is small (i.e. where $j \leq \pi$) the coupling is weak, but when $j \gg \pi$ the coupling is strong.

4. FEL Gain and Phase Space Plots

a. Gain

The electrons will gain and lose the same amount of energy when at resonance according to equations 2.13 and 2.20. This is undesirable since no energy would thereby be transferred into the optical beam. In order to have gain, the electrons must be slightly off resonance. Optimally they have an initial phase velocity of $v_0 \approx 2.6$ for weak fields, resulting in a gain of $G \approx 0.135 j$. Gain is defined as

$$G = \frac{(|a(\tau)|^2 - a_0^2)}{a_0^2}, \quad (2.22)$$

where a_0 is the initial optical field strength and $a(\tau)$ is the field strength along the undulator. As the optical field reaches a maximum at saturation in strong fields the gain will be reduced to equal the resonator's output coupling.

b. Phase Space Plots

A plot of the evolution of the electrons in phase space is a useful method to display the effectiveness of an FEL. As shown in Figure 5 the phase space is plotted as the phase velocity versus the electron phase. This shows a case where the electrons start with an initial phase velocity of $\nu_0 = 0$, which is undesirable in a working FEL, since an equal amount of electrons gain and lose energy so that no net energy is transferred to the optical beam. This can be seen in Figure 5 by noting that an equal number of electrons raise their phase velocity as those that lower their phase velocity. The electrons begin with an initial phase velocity of zero shown in yellow on the figure and evolve through the undulator and their final positions in phase space are plotted in blue. The electron phase velocity is simply related to the electron energy by $\Delta\gamma/\gamma \approx \Delta\nu/4\pi N$ [6, b].

In order to have optimal gain, the initial phase velocity should be $\nu_0 \approx 2.6$, which results in a gain of about $G \approx 0.135j$ while the optical fields are weak. In the case of optimal gain, instead of the electrons bunching at the phase $\zeta + \phi \approx \pi/2$ as in Figure 5 they will bunch at $\zeta + \phi \approx \pi$. As a result more electrons will lose phase velocity than gain phase velocity. When the optical field becomes strong, the electrons will reach a point where they no longer lead to as much optical growth and this is called “saturation”.

The gain and phase of the optical beam is plotted on the right in Figure 5. Both the gain and phase plots are plotted versus the dimensionless time, where $\tau = 0 \rightarrow 1$ represents the electrons traveling from the beginning to the end of the undulator. As can be seen in Figure 5 there is very little gain since the electrons are on resonance, and the phase shift in the light is substantial.

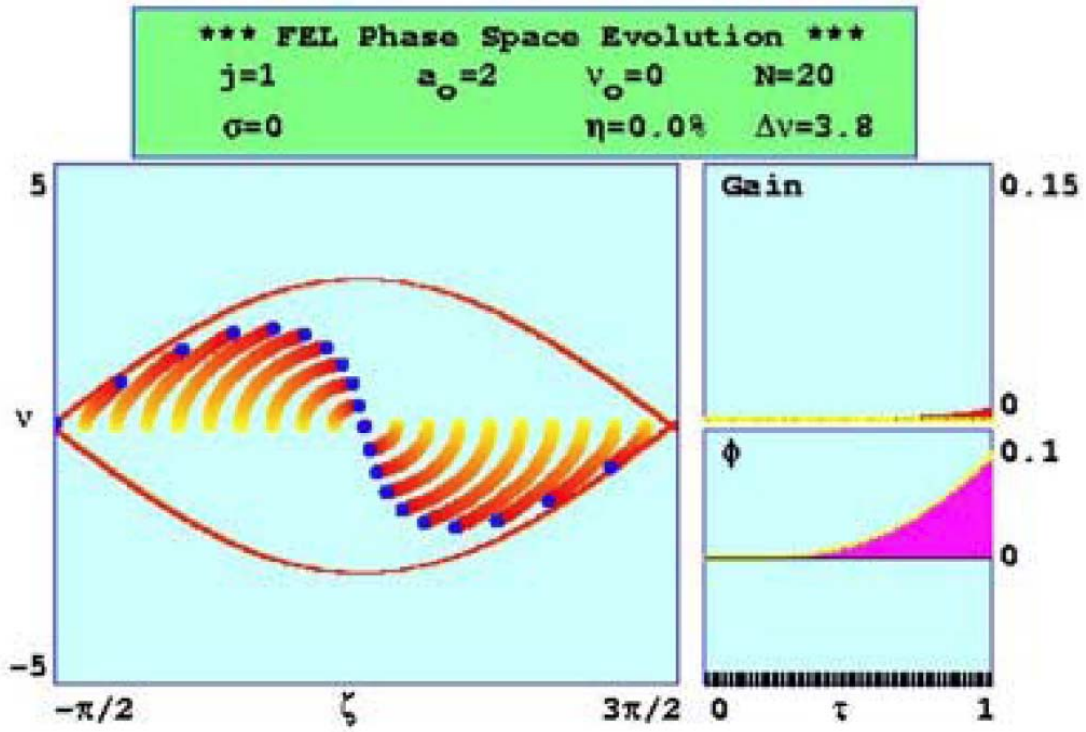


Figure 5. Phase space plot of electron evolution [From 6, a].

THIS PAGE INTENTIONALLY LEFT BLANK

III. ENERGY REQUIREMENTS

The free electron laser will be part of a future all-electric ship, where all the ship's systems including propulsion will use the same power. This will enable the power to be distributed as needed for different scenarios. For instance, the power can be transferred from the propulsion system to the FEL if the ship comes under attack from enemy missiles. In this chapter, the power requirements of the FEL will be addressed as well as the FEL efficiency and the methods of generating the required power.

A. ESTIMATED POWER REQUIREMENT

The FEL requires a substantial amount of electrical power to operate, and because of this it will be necessary to direct power from other systems to the FEL when it is running. The power required depends on the desired output power of the FEL, but there are some values which are fixed, such as the cryoplant. The cryoplant requires an input power of about 0.5MW as shown in Figure 6. The FEL shown projects an output of about 3MW of optical power and will require more RF power than a 1MW FEL. Figure 6 also shows the power for the auxiliary systems, such as guiding magnets and other electronics that monitor and align the electron and optical beams, which will require a total power of about 1MW [7]. These two power requirements are fixed for all FELs designed for weapons and set a minimum power required for the FEL.

To accommodate various output powers, the RF power must be capable of increasing to generate higher electron beam energy. The RF system requires 11.4MW in the 3MW laser in Figure 6, which is most of the power consumed for the FEL [7]. As can be seen in Figure 6, much of the RF power goes into the SRF injector. The reason for this is that the SRF injector does not have recirculation of the electron beam while the SLINAC does. The recirculation of the electron beam allows the energy of the electron beam to be recycled and transferred back into the RF field. If recirculation were not present, the FEL would require about 100MW of power for the SLINAC.

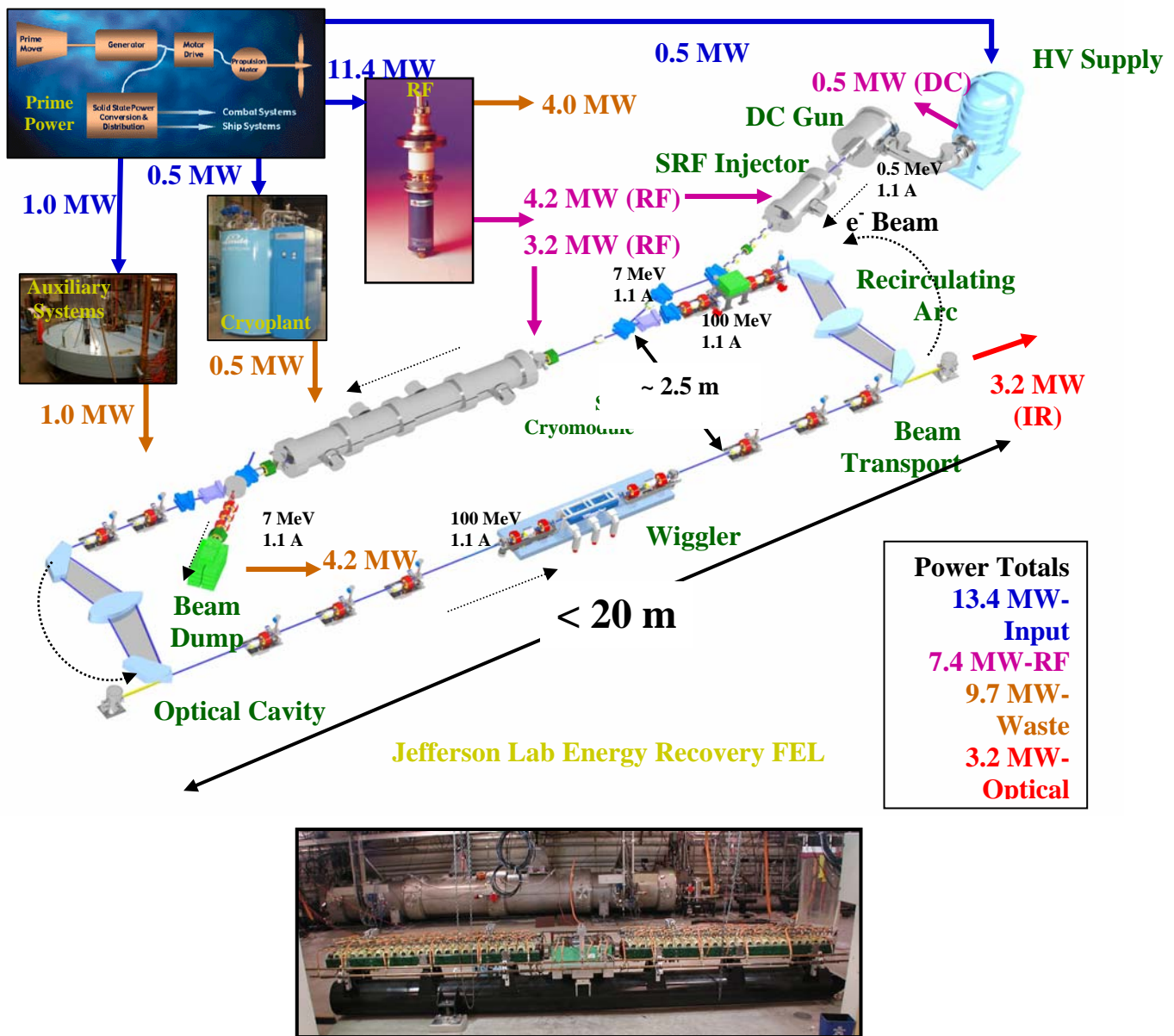


Figure 6. 3MW FEL with power requirements for each system [From 7].

The DC gun requires energy of about 0.5MW, as seen in Figure 6 [7]. This makes the total energy requirements of the entire FEL to be about 13.4MW for the 3MW FEL. As shown in Figure 6, the output of this FEL is 3.2 MW while the rest, 9.7MW, is converted to heat [7]. The efficiency for this particular FEL is also about 23%. In the next section, the FEL efficiency will be examined in greater detail.

B. EFFICIENCY OF THE FEL

The free electron laser has the capability of very high efficiency compared to other types of lasers. The reason for this is partly due to the high power transfer efficiency between free electrons in klystrons and inductive output tubes (IOTs). In this section the efficiencies of klystrons and IOTs will be examined as well as calculations to estimate the efficiency of the FEL.

1. Klystron and IOT Descriptions

The klystron is an efficient method of amplifying RF signals, one which has been in use for decades in communications. It has also been in wide use to create RF power for linear accelerators. In fact at SLAC in Stanford, klystrons have been in use since the late 1940's, and many of the advances in klystron design have been made there since the Varian brothers invented them at Stanford in 1937 [8]. Figure 7 shows a two cavity klystron. The klystron operates by sending an electron beam from a cathode through a vacuum tube to a beam dump at the end. There is an input frequency in the first cavity that is transmitted to a grid which the electrons pass through. The electrons are accelerated or decelerated by the input RF frequency, creating a spread of electron velocities. As the electrons pass through a drift space they will bunch at the same frequency of the input RF due to the differences in their velocities. When the electrons reach the catcher cavity, they create an RF field which is greatly amplified from the original input power. This output RF power will then be sent through a waveguide to the FEL accelerator.

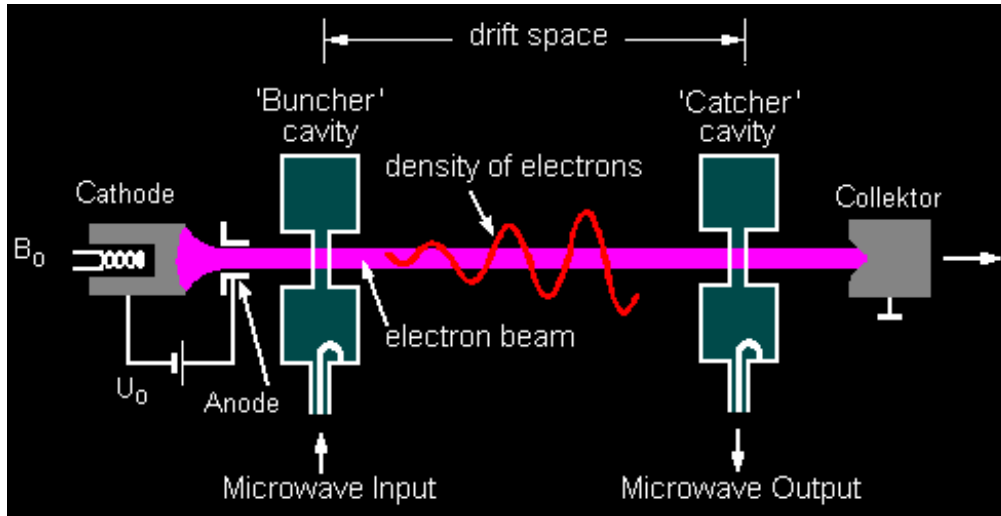


Figure 7. Two cavity klystron [From 9].

The two cavity klystron, Figure 7, is the simplest type; however for greater efficiency the FEL would use a multicavity klystron. In a multicavity klystron, shown in Figure 8, the electron beam will pass an input cavity, as in the two cavity case. The electrons will then drift to intermediate cavities which are designed to resonate at the desired frequency. As the electrons enter the intermediate cavity they will set up small oscillations and these will produce an oscillating voltage across the cavity, which will further bunch the electrons in the beam. This type of klystron is the most common in use and its efficiency is about 65%. While it is possible to have a higher efficiency it is difficult due to RF instability and the high cathode voltage required [10].

Klystron technology is very well developed, and they are very reliable. Their use in accelerators and FELs has a long and effective history. They have been used on ships for radar as well as being used for satellite communications. Also the mechanism of using a beam of free electrons is similar in principle to the FEL.

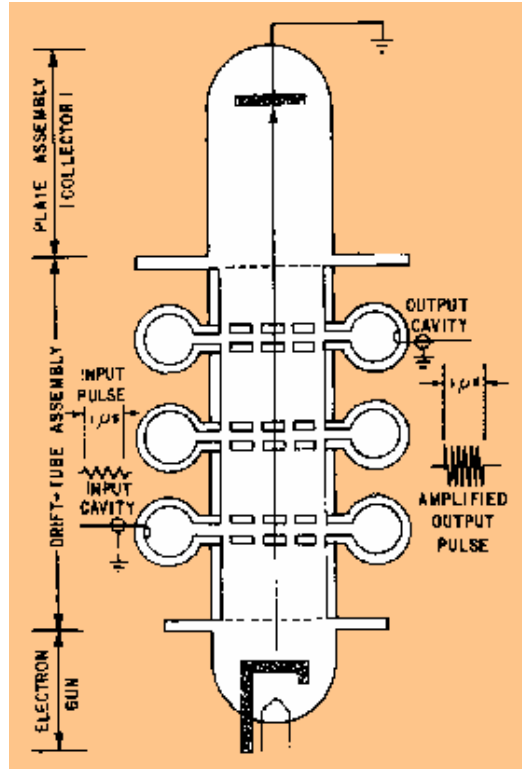


Figure 8. Multicavity klystron [From 11].

An alternative to the klystron for the RF power needed for the FEL is the inductive output tube or IOT, a cross section of which is shown in Figure 9. The IOT operates on a similar principle to the klystron in the sense that it also bunches electrons to amplify an RF signal. IOTs are also in wide use in UHF transmitters due to their efficiency and smaller size. The control grid in front of the cathode controls the electrons leaving the cathode. The control grid's voltage is modulated at the RF frequency but has a negative DC bias. Due to this modulation, the electrons will leave the cathode in bunches and at varying velocities, just as when the electron in the klystron passes the input cavity. The electrons will then drift to an output window where the RF power is carried away through a wave guide.

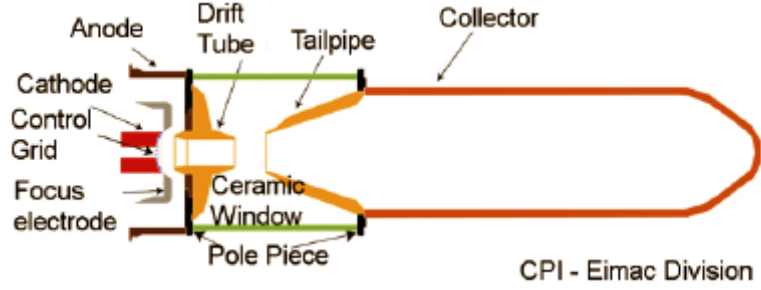


Figure 9. IOT cross section [From 12].

While the IOT was first created at around the same time as the klystron, it has not been in wide use until the last couple of decades. The IOT, with efficiencies above 70% being shown in UHF applications, is slightly more efficient than the klystron [12]. This increase in efficiency makes it a desirable choice for the FEL since the power which will be used for creating the RF power is very high, a total of 11.4MW is used for a 3MW FEL. The IOT is also smaller which is an added advantage on a ship.

2. FEL Efficiency Calculation

The 3MW FEL design has an anticipated efficiency of around 23%. The wall plug efficiency is defined as

$$\eta_{WP} = \frac{P}{P_{in}}, \quad (3.1)$$

where η_{WP} is the wall plug efficiency, P is the output power of the laser and P_{in} is the total power used by the FEL. As noted before, there are the fixed powers of the cryoplant and auxiliary systems which are independent of the desired output power. This is $P_0 = P_{cryo} + P_{aux} \approx 1\text{MW}$. The input power also includes the power necessary for the injector and accelerator, and must equal the power leaving the laser system in the beam dump $I\langle V' \rangle$ and P , so that

$$P_{in} = (I\langle V' \rangle + P) / \eta_{RF} + P_{cryo} + P_{aux}, \quad (3.2)$$

where I is the current of the electron beam, $\langle V' \rangle$ is the average voltage of electrons at the dump, η_{RF} is the efficiency of the klystron or IOT, and P_{cryo} and P_{aux} are the powers to the cryoplant and auxiliary systems. The power going into the system is the sum of the power required for the injector, the power of the accelerator minus the power recovered from recirculation, and the fixed powers consumed by the cryoplant and auxiliary systems. The value of P / η_{RF} appears because, although most of the power is returned to the accelerator through recirculation, the amount of power that is sent out through the optical beam must be replaced by the klystrons or IOTs.

The total optical power extracted from the FEL is an extraction percentage of the power of the electron beam going through the undulator. So the optical beam has a power of

$$P = \eta IV , \quad (3.3)$$

where η is the extraction of the FEL and V is the voltage of the electrons arriving at the undulator. The value of the injector voltage is typically much less than the accelerator voltage since $V_{inj} \approx 5 - 7$ MV and $V \approx 75 - 100$ MV.

Substituting the value for the input power into the equation for the wall plug efficiency, simplifying this using equation 3.3 and setting $P_0 = P_{cryo} + P_{aux}$ an equation for efficiency in terms of power can be obtained:

$$\eta_{WP} = \frac{P}{P_0 + P[\langle V' \rangle / (V\eta) + 1] / \eta_{RF}} . \quad (3.4)$$

The value of the extraction can also be estimated to be between $1/(2N)$ and $1/N$, so an intermediate value of $\eta \approx 2 / (3N)$ is chosen for the estimate [6, c].

The values of the fixed power can be estimated to be about $P_0 \approx 1$ MW and the efficiency of the klystrons or IOTs to be $\eta_{RF} \approx 60\%$ [7]. These values when substituted into equation 3.4 give an equation for the wall plug efficiency to be about

$$\eta_{WP} \approx \frac{P}{1MW + 5P} \quad (3.5)$$

This agrees with data from AES, which shows that the efficiency of an FEL increases with the output power, with a 100kW laser having about 5% efficiency and a 3MW laser about 23%. As can be seen from equation 3.5, as $P \rightarrow \infty$ the upper limit on efficiency is about 20%. It is also clear that for an FEL with an output below the fixed powers for the cryoplant and the auxiliary systems, the efficiency will be much lower.

C. POWER GENERATION

In the all-electric ship the power system will be integrated so that the power can be shared or readily transferred from one system to another. Since the propulsion will also be electrically powered, the total electric power on the ship will significantly exceed the required 15-20MW necessary to operate the FEL.

Current day vessels such as the Navy's guided missile destroyers have 75MW in mechanical power for propulsion. The FEL could use the power coming directly from the ship, but a powerful generator would have to be added and other systems would have to sacrifice some of their power during FEL operations.

Another solution is to store the power in a bank of capacitors or flywheels. This would require a smaller continuous power but enable the FEL to be operated without the need to cut power to other systems. The drawback with this solution is that the FEL could only operate for short periods of time before the energy would be exhausted.

IV. SHIP MOTION AND FEL TOLERANCE

In order to determine if the FEL will successfully operate on the all-electric ship, the motion of the ship and the motion tolerances of the FEL must be explored. The ship's motion will be examined so that there is a base to start from when looking at the FEL tolerance. These will be determined using computer simulations. In the next chapter, after comparing the tolerance with the ship's motion, we will examine how to diminish the motion through active alignment, isolation, and damping.

A. SHIP MOTION

Ships will behave differently due to differences in their designs. The physical dimensions of the ship as well as its mass will influence how it behaves in the ocean. Each all-electric ship will have its own unique motion, but by examining how current ships of similar size behave we can approximate the relevant vibrations and flexing.

The ship motion of a FFG-7 is given in Table 1, which shows the maximum amplitude and the period. The FFG-7 class of ships is primarily an anti-submarine warfare platform that is about 450ft long and displaces about 4,100tons. The conditions shown in Table 1 range from "normal" where all the ship systems are operating as designed, "reduced" where the ship has lost a capability such as propulsion, and "withstand" conditions, which are the extreme conditions the ship will undergo. The motions in Table 1 all have a long period relative to the time which the FEL comes to equilibrium operation. This means that these long period motions will not affect the FEL physics, but will need to be taken into account for engineering the systems, such as how the liquid helium is stored and how the FEL is mounted. Vibration, however will affect the FEL in a more significant way. If certain parts of the FEL system move far enough out of their proper location, then the FEL performance can be reduced, even to the extent of "turning off." The extreme result could be oscillations in power, wavelength, or beam position. This study and subsequent research will determine how to isolate the FEL and make active corrections to critical parts.

Table 1. FFG-7 ship motions maximum amplitude minimum period.

Sinusoidal	Normal Conditions	Operating	Reduced Conditions	Operating	Withstand Conditions	
	Amplitude (deg.)	Minimum Period (sec)	Amplitude (deg.)	Period (sec)	Amplitude (deg.)	Period (sec)
Roll	± 25	8.5	± 35	8.5	± 45	8.5
Pitch	± 5	7	± 8	7	± 15	7
Yaw	± 2.5	7	± 4	7	± 7.5	7

The vibrations which the FEL must withstand to be used on board a ship are given in MIL-STD-167-1A. Typical ships have vibrations from zero Hz to about 33Hz, and some vessels have vibrations up to around 50Hz. The test requires that the FEL operate at frequencies from 4Hz up to 33Hz in intervals of 1Hz for five minutes at each frequency. These frequencies correspond to long times compared to the amount of time that electron and optical pulses spend in the FEL. The amplitude of the ship vibration is significant however, with a maximum amplitude of about 0.75mm and is shown at various frequencies in Table 2.

Table 2. MIL-STD-167-1A vibration displacement criteria for variable frequency test

Frequency Range (Hz)	Vibration Table Single Amplitude (inch)
4 to 15	0.030 ±0.006
16 to 25	0.020 ±0.004
26 to 33	0.010 ±0.002

Since the FEL must operate at these frequencies and displacements, the tolerance of the FEL to misalignment must be examined. By determining how sensitive the FEL is to vibration and comparing this with the data from the ship motion we can determine whether it is reasonable to expect that the vibration can be rendered acceptable through isolation and active alignment.

B. FEL TOLERANCE

In this section, the tolerance of the FEL to misalignments in both the electron beam and the mirrors will be explored. This is done using simulations developed at NPS by Professors Colson and Blau. In the simulations, the misalignment is the input and the corresponding extraction of the FEL is determined. From the extraction, the output power of the FEL may be calculated and compared to the desired output.

1. FEL Designs

The simulations of the high power FELs will include one megawatt (at 1.6microns) and three megawatts (at both one micron and 1.6microns) output. Other lower power designs are also simulated. The parameters of the high power FEL designs are shown below in Tables 3 through 8.

Table 3 shows the properties of the electron beam for the oscillator configurations of each power. The first value E_b is the energy of the electron beam in MeV when it passes through the undulator. The value q_{bunch} is the charge of the electron bunch in nano-Coulombs. The electron beam radius in millimeters is r_b and the duration of the electron pulse at full width at half of its maximum (FWHM) is t_b and is in pico-seconds. The pulse repetition frequency is the frequency of the electron pulses and is given in MHz. The length of the electron pulse also at FWHM is l_b in centimeters. The Lorentz factor of the electron beam is γ and from equation 2.8 is one of the factors determining the optical wavelength. The peak and average currents are given as I_{peak} in amps and I_{avg} in milli-amps respectively. The emittance of the electron beam describes how the electron bunch will spread in both the longitudinal and the transverse directions. The normalized and longitudinal emittances are $emitt_n$ in millimeter milli-radians and $emitt_l$ in keV pico-seconds. The energy spread of the electrons describes the percent difference between the maximum and minimum energies of the electrons and is d_{dog} . The angular spread of the electron beam is d_{theta} measured as a root mean square in milli-radians and describes the angle that the electron beam spreads through the undulator. The beam density ρ in cm^{-3} describes how compact the pulse of electrons is

while entering the undulator. The power of the electron beam is P_b and given in MW. The values that are calculated are shown with the formula used to determine them to the right of their description.

Table 3. Electron beam properties for oscillator FEL designs.

		1MW OSC '07	3 MW OSC '07	3 MW OSC '07
		1.6 micron	1.6 micron	1 micron
	ELECTRON BEAM PARAMETERS	FORMULA		
E_b	Beam energy (MeV)		80	105
q_{bunch}	Bunch charge (nC)		0.8	1.2
r_b	Beam radius, rms (mm)	$W_0/(2*\sqrt{2})$	0.08	0.08
t_b	Pulse duration, FWHM (ps)		1	1
prf	Pulse rep frequency (MHz)		703	703
l_b	Pulse length, FWHM (cm)	$1E-12*t_b*c$	0.03	0.03
γ	Lorentz factor	$(E_b+0.511)/0.511$	158	206
I_{peak}	Peak current (A)	$q_{bunch}*1000/t_b$	800	1200
I_{avg}	Average current (mA)	$q_{bunch}*prf$	562	844
ϵ_{mitn}	Normalized emittance (mm mrad)	$1+10.5*ATAN((q_{bunch}/2)^{1.5})$ DC GUN	3.6	5.6
ϵ_{mitl}	Longitudinal emittance (keV ps)	$35+25*ATAN((2*q_{bunch}/3)^{1.5})$	44	51
$dgog$	Beam energy spread (%)	$0.1*2.35*\epsilon_{mitl}/(E_b*t_b)$	0.13	0.11
$d\theta$	Beam angular spread, rms (mrad)	$\epsilon_{mitn}/(\gamma*r_b)$	0.29	0.34
ρ	Beam density (1/cm ³)	$I_{peak}*3E9/(e*2*PI*r_b*r_b*0.01*c)$	4.1E+14	6.2E+14
P_b	Beam average power (MW)	$E_b*I_{avg}*0.001$	45	89

Table 4 shows the values of the electron beam for the amplifier FELs. The differences in these designs are the beam radius, r_b , which is about 50% wider. Because of this the electron beam angular spread, $d\theta$, is less to keep the normalized emittance fixed and the electron beam density, ρ , is also decreased. The reason for having a smaller angular spread in the amplifier FEL is so the electrons do not spread to the edges of the undulator since it is much longer than that in the oscillator FEL.

Table 4. Electron beam properties for amplifier FEL designs.

		1MW AMP '07	3MW AMP '07	3MW AMP '07
ELECTRON BEAM PARAMETERS		1.6 micron	1.6 micron	1 micron
FORMULA				
Eb	Beam energy (MeV)	80	105	105
qbunch	Bunch charge (nC)	0.8	1.2	1.2
rb	Beam radius, rms (mm)	$\text{SQRT}(\text{emitn} \cdot L / (4 \cdot \gamma)) / 10$		
tb	Pulse duration, FWHM (ps)	1.0	1.0	1.0
prf	Pulse rep frequency (MHz)	703	703	703
lb	Pulse length, FWHM (cm)	$1 \text{E} - 12 \cdot \text{tb} \cdot c$		
gamma	Lorentz factor	$(\text{Eb} + 0.511) / 0.511$		
lpeak	Peak current (A)	$\text{qbunch} \cdot 1000 / \text{tb}$		
lavg	Average current (mA)	$\text{qbunch} \cdot \text{prf}$		
emitn	Normalized emittance (mm mrad)	$1 + 10.5 \cdot \text{ATAN}((\text{qbunch} / 2)^{1.5})$ DC GUN		
emitl	Longitudinal emittance (keV ps)	$35 + 25 \cdot \text{ATAN}((2 \cdot \text{qbunch} / 3)^{1.5})$		
dgog	Beam energy spread (%)	$0.1 \cdot 2.35 \cdot \text{emitl} / (\text{Eb} \cdot \text{tb})$		
dtheta	Beam angular spread, rms (mrad)	$\text{emitn} / (\gamma \cdot \text{rb})$		
rho	Beam density (1/cm ³)	$\text{lpeak} \cdot 3 \text{E} 9 / (e \cdot 2 \cdot \text{PI} \cdot \text{rb} \cdot \text{rb} \cdot 0.01 \cdot c)$		
Pb	Beam average power (MW)	$\text{Eb} \cdot \text{lavg} \cdot 0.001$		

Table 5 shows the properties of the undulator in the FEL oscillator designs. The value of the undulator period, λ_0 measured in centimeters, gives the length of one period of the magnetic field of the undulator. The number of periods in the undulator is N. The undulator gap gives the spacing between the magnets of the undulator and is in centimeters. The peak magnetic field in the undulator is B_{peak} and given in Teslas. The root mean square value of the magnetic field in the undulator is also given in Teslas and is B_{rms} . The dimensionless undulator parameter using the root mean square magnetic field is K and along with the undulator period and the Lorentz factor determines the optical wavelength. The length of the undulator, L, is in centimeters.

Table 5. Undulator properties for oscillator FEL designs.

		1MW OSC '07	3 MW OSC '07	3 MW OSC '07
UNDULATOR PARAMETERS		1.6 micron	1.6 micron	1 micron
FORMULA				
lambda0	Undulator period (cm)	2.70	3.05	3.05
N	Number of periods	20	18	18
gap	Undulator gap (cm)	1	1	1.25
Bpeak	Undulator peak magnetic field (T)	$3.7 \cdot \text{EXP}(-(\text{gap} / \lambda_0) \cdot (4.65 - 1.25 \cdot (\text{gap} / \lambda_0)))$		
Brms	Undulator magnetic field, rms (T)	$\text{Bpeak} / \text{SQRT}(2)$		
K	Undulator parameter, rms	$e \cdot \text{Brms} \cdot 1 \text{E} 4 \cdot \lambda_0 / (2 \cdot \text{PI} \cdot m \cdot c^2)$		
L	Undulator length (cm)	$N \cdot \lambda_0$		

Table 6 gives the undulator properties for the amplifier FEL designs. The differences with the oscillator FELs are the increased number of periods, N, and the undulator length L. The reason for this is that the amplifier needs a longer undulator with more periods in order to reach extractions that give the desired amount of output power in a single pass.

Table 6. Undulator properties for amplifier FEL designs.

UNDULATOR PARAMETERS		FORMULA	1MW AMP '07	3MW AMP '07	3MW AMP '07
			1.6 micron	1.6 micron	1 micron
λ_0	Undulator period (cm)		2.70	3.05	3.05
N	Number of periods		100	100	100
gap	Undulator gap (cm)		1.00	1.00	1.25
B_{peak} *	Undulator peak magnetic field (T)	$3.7 \cdot \exp(-(\text{gap}/\lambda_0)^{4.655-1.25 \cdot (\text{gap}/\lambda_0)})$	0.78	0.92	0.68
B_{rms}	Undulator magnetic field, rms (T)	$B_{peak}/\sqrt{2}$	0.55	0.65	0.48
K	Undulator parameter, rms	$e \cdot B_{rms} \cdot 10^4 \cdot \lambda_0 / (2 \cdot \pi \cdot m \cdot c^2)$	1.39	1.85	1.36
L	Undulator length (cm)	$N \cdot \lambda_0$	270	305	305

Table 7 shows the parameters for the optical cavity in the oscillator FEL designs. The length of the cavity from mirror to mirror is S and is in meters. The Rayleigh length, which determines how quickly the optical beam expands, is Z0 and is in centimeters. Lowering the Rayleigh length causes the optical beam to have a smaller radius at its waist and a larger radius at the mirrors and thus can be varied to lower the intensity on the mirrors. The mirror loss per pass, loss, is a percentage of the light leaving the oscillator. The optical wavelength, λ , is in microns. The waist radius, W0 measured in centimeters, is where the optical beam's radius is the smallest and is measured so that the optical field amplitude drops to 1/e of its maximum. The optical radius at the mirrors is also measured at its 1/e value and is Wmir measured in centimeters. The quality factor, Qn, is the reciprocal of the mirror loss and describes the ratio of optical energy in the oscillator to the energy leaving; lowering this value reduces the optical energy inside the cavity. The predicted extraction, eta, is a rough estimate of the percentage of electron beam energy that will be converted to output optical energy. The predicted output power, Pout in MW, uses the estimate of the extraction and the electron beam energy to estimate

the output power of the FEL. The intensity of the optical energy on the mirrors is I_{mir} and is in kW/cm^2 . The limit of intensity on the mirrors is about $200\text{kW}/\text{cm}^2$ before they will become damaged.

Table 7. Optical cavity specifications for oscillator FEL designs.

		1MW OSC '07	3 MW OSC '07	3 MW OSC '07
OPTICAL CAVITY PARAMETERS	FORMULA	1.6 micron	1.6 micron	1 micron
S	Cavity length (m)	20	20	20
Z0	Rayleigh length (cm)	5	5	5
loss	Mirror losses per pass (%)	50	50	50
lambda	Optical wavelength (microns)	1.6	1.6	1.0
W0	Mode waist radius, 1/e (mm)	10*SQRT(Z0*lambda*0.0001/PI)	0.16	0.16
Wmir	Mode radius at mirrors, 1/e (cm)	0.1*W0*SQRT(1+1E4*(S/(2*Z0))^2)	3.2	3.2
Qn	Quality factor	100/loss	2.0	2.0
eta	Predicted extraction (%)	100/(2*N)	2.5	2.8
Pout	Predicted output power (MW)	.01*eta*Pb	1.1	2.5
Imir	Optical intensity at mirrors (kW/cm^2)	1000*Pout*Qn/(PI*Wmir^2)	70	155

Table 8 shows the values of the optics for the amplifier FEL designs. The value of the average power of the seed laser is P_{inavg} in Watts. The duration of the optical pulses from the seed laser is t_{in} in pico-seconds. The peak optical power from the seed laser is P_{in} in MW. The energy of the optical beam from the seed laser is E_{in} measured in micro-Joules. The electric field strength of the optical beam from the seed laser measured in statvolts/cm is E_{fieldin} . The distance to the first optic from the undulator is S measured in centimeters. The Rayleigh length, Z_0 , is greater than in the case of the oscillator so the optical beam will not spread as rapidly. The waist radius, W_0 , is larger and the optical beam radius at the mirror, W_{mir} , is smaller than in the oscillator due to the larger Rayleigh length. The extraction estimate, η_{ahg} , gives an estimate of the percentage of the electron beam energy that will be converted to optical energy in a high gain FEL. The predicted output power, P_{out} , uses the high gain extraction to estimate the output power of the laser. The optical intensity on the first mirror is higher for all the amplifier designs and also exceeds the limit of $200\text{kW}/\text{cm}^2$.

Table 8. Optical specifications for amplifier FEL designs.

		1MW AMP '07	3MW AMP '07	3MW AMP '07
OPTICAL PARAMETERS	FORMULA	1.6 micron	1.6 micron	1 micron
P_{inavg}	Average input power from seed laser (W)	100.0	100.0	100.0
t_{in}	Input optical pulse duration (ps)	2.0	2.0	2.0
P_{in}	Peak input power from seed laser (MW) $P_{inavg}/(prf*t_{in})$	0.07	0.07	0.07
E_{in}	Input optical pulse energy (μ J) $P_{in}*t_{in}$	0.14	0.14	0.14
$E_{fieldin}$	Input electric field strength (statvolts/cm) $0.5*\sqrt{8E13*P_{in}/(c*(0.1*W0)^2)}$	196	170	170
S	Distance to First Optic (cm)	1000	1000	1000
$Z0$	Rayleigh length (cm) $100*PI()*W0^2/\lambda$	24	33	51
λ	Optical wavelength (microns) $\lambda0*(1+K^2)/(2*\gamma^2)*1E4$	1.60	1.58	1.02
$W0$	Mode waist radius, 1/e (mm) $2*r_b/\sqrt{F}$	0.35	0.41	0.41
W_{mir}	Mode radius at mirror, 1/e (cm) $0.1*W0*\sqrt{1+((S-L)/Z0)^2}$	1.1	0.9	0.6
η	Predicted extraction (%) $100/(2*N)$	0.5	0.5	0.5
η_{ahg}	Predicted extraction, high gain (%) $100*(j_{lin}*F/2)^{(1/3)}/(8*N)$	1.6	1.7	1.4
P_{out}	Predicted output power (kW) $10*\eta_{ahg}*P_b$	739	1465	1236
I_{mir}	Optical intensity at mirror (kW/cm ²) $P_{out}/(PI()*W_{mir}^2)$	210	627	1263

Using the information from the above tables the dimensionless values used by the computer simulations are calculated. The computer simulations of the FEL designs show the ability to meet the desired laser power. Figure 10 below shows a sample computer simulation for the one-megawatt design. In this figure notice that in the phase space diagram (right) the electrons bunched well and lost energy to the optical field. This means that the optical energy is being amplified. Also, the plot to the left of the phase space shows the optical intensity in the undulator, and in this case the electron pulses in red overlap the optical energy in blue. The left side of the figure shows where the electrons and optical beam enter the undulator and also has a curve in yellow of the optical field amplitude at the entrance of the undulator. The right side shows the exit of the undulator. The curves in pink show a Gaussian for reference. For this case, the laser had an extraction of 3.4% and an output of 1.5MW. Similarly, the three-megawatt laser designs and the amplifier designs were run and give the power outputs in Table 9. The simulations for the most part met the goal of the design except for the one-micron FEL designs which did not have sufficient extraction to reach the desired output powers.

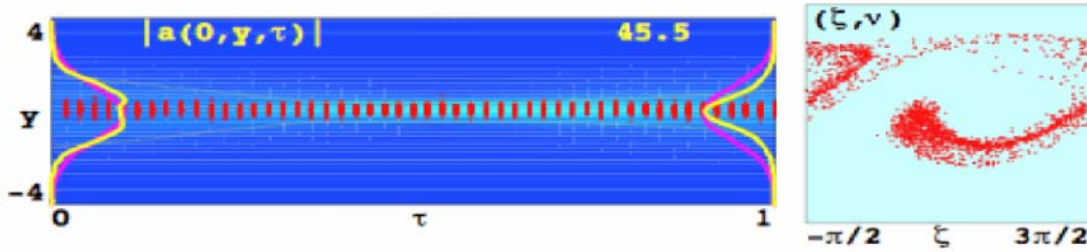


Figure 10. One-megawatt oscillator FEL design at 1.6micron wavelength.

Table 9. Power outputs of high power FEL designs.

FEL Design	Output Power (MW)	
	Oscillator	Amplifier
1MW @ 1.6micron	1.5	1.6
3MW @ 1.6micron	3.2	3.2
3MW @ 1micron	2.8	1.7

2. Electron Beam Shift

Due to vibrations the electron beam may shift off-center and thus not fully interact with the optical beam through the undulator. This is a concern in the oscillator since the Rayleigh length is short and the radius of the optical beam is small (about 0.2mm) in the center of the undulator. Alignment is a concern for the amplifier because a small electron beam must stay aligned with a small optical mode over a longer undulator. To determine how much of a problem this may be, simulations of the FEL are run with varying amounts of electron beam shift.

These simulations have been done using high power FEL designs as well as for the FEL at Jefferson Lab. As expected, the lateral displacement of the electron beam does cause the extraction and gain of the FEL to decrease, but the result is not catastrophic. In fact, the FEL will continue to operate at high power even with a significant displacement in the electron beam. In Figure 11, the extraction of a 100kW FEL amplifier design is shown as a function of the electron beam displacement. As can be seen, the FEL extraction decreases as the electron beam shift increases. The total energy of the electron beam of this particular design is 11MW, and since the initial extraction is about 1.7% the optical output is initially about 185kW. However, the FEL

will still output 100kW at an extraction of about 0.9%, meaning that a displacement of about 0.4mm is acceptable for this design. This means that a rather large electron beam displacement of 0.4mm causes a reduction of about 45% in the total optical power. Results similar to this have been simulated for both the high power FEL designs as well as the Jefferson Lab FEL.

While this displacement is about half of the maximum displacement expected for ship vibrations (discussed in the previous section), it should be correctible by isolation and active systems to steer the electron beam.

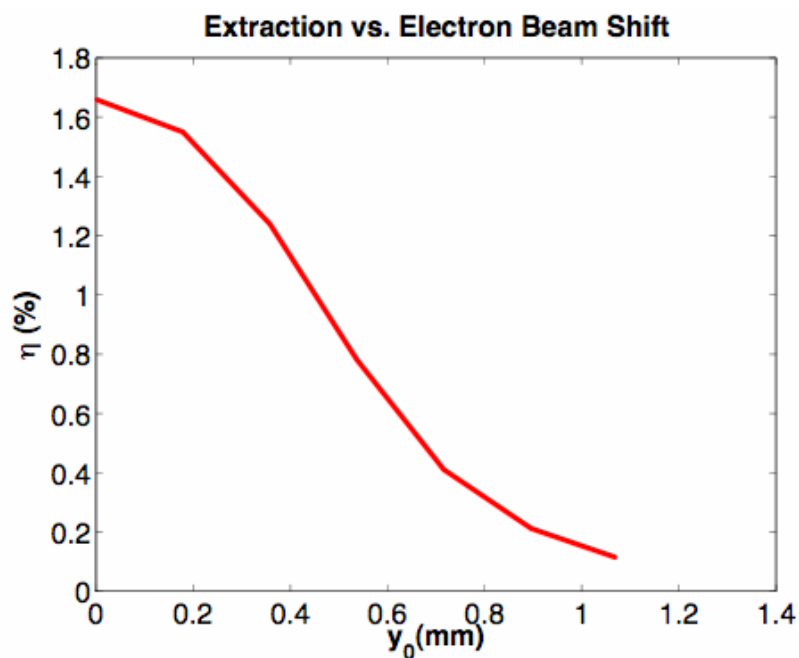


Figure 11. Extraction versus electron beam shift for 100kW FEL amplifier design.

3. Electron Beam Tilt

Ship vibrations may also cause the electron beam to tilt at an angle off the axis of the optical beam. This will also be a problem due to the fact that the electrons and optical energy will not overlap completely, and the extraction of the FEL will be reduced. To examine the effects of electron beam tilt, simulations were run to see the extent to which the FEL could tolerate an electron beam tilt and still have an acceptable extraction. The results of the electron beam tilt are of a similar scale to the electron beam shift. The

simulations show that the electron beam tilt must be kept within milliradians in order to have the desired extraction levels for the FEL oscillator.

The FEL is relatively insensitive to electron beam shift and tilt. The reason for this is that the optical beam will try to “follow” the electron beam, since the electron beam is amplifying the optical energy. An example of this can be seen in Figure 12 where the electron beam in red is tilted through the oscillator and the optical beam in light blue roughly follows the same path. The electron beam and optical mode are shown inside the undulator length. At each end of the undulator, the optical mode is shown in yellow.

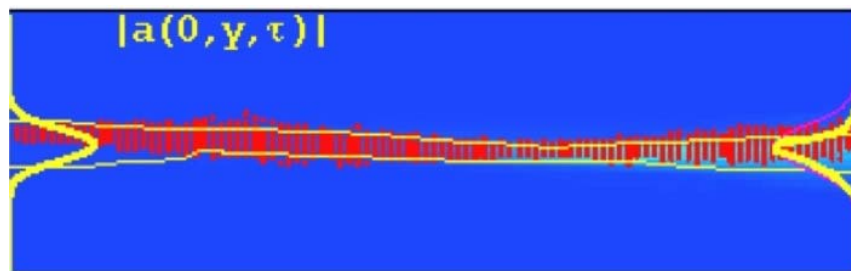


Figure 12. Optical energy in an oscillator FEL with an electron beam tilt.

4. Mirror Shift

In the computer simulations “mirror shift” means that the axis of one mirror is displaced off of the axis of the undulator. This is only a problem in the oscillator FEL since the amplifier does not have mirrors to store the optical energy. The analogous problem for the FEL amplifier could be a misaligned seed laser. The simulations show that the effects of mirror shift are much greater than the effects of electron beam shifts. Mirror shifts on the order of magnitude of tens of microns are the limit of acceptable displacements. Figure 13 below shows how, while the electron beam remains straight, the optical beam is off axis due to the mirror shift. The mirror shift thus reduces the amount of interaction between the optical and electron beams, so the extraction is greatly reduced. The reduced extraction can be seen in Figure 14 where the extraction falls to half of its original value at about 80microns of mirror displacement. In this case the extraction initially increases with mirror shift; this may be due to over-bunching when

there is no mirror shift causing the electrons to take back some energy from the optical beam. When a small mirror shift occurs the electrons then do not over-bunch and the extraction increases.

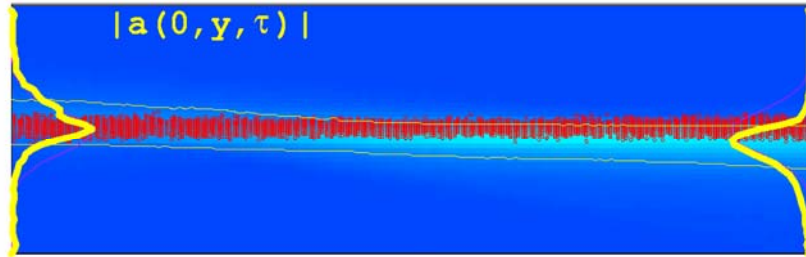


Figure 13. Optical energy in an oscillator FEL with a mirror shift.

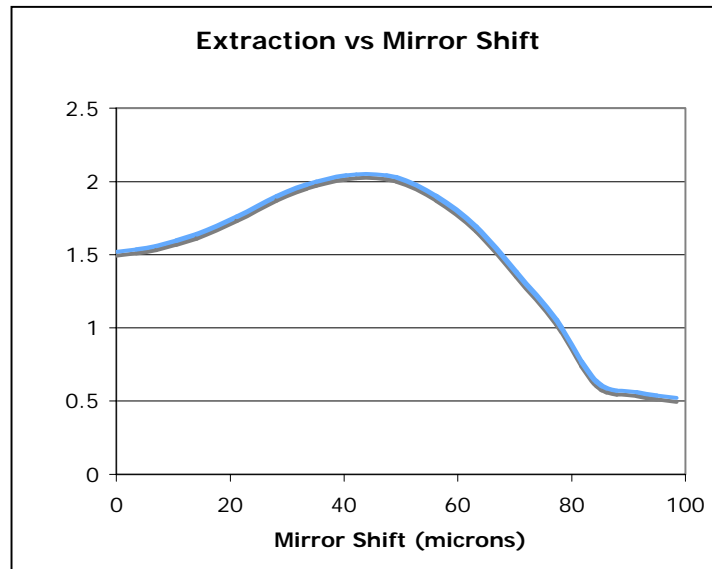


Figure 14. Extraction versus mirror shift in Jefferson Lab FEL.

5. Mirror Tilt

As with mirror shifts, the FEL is also sensitive to mirror tilt. “Mirror tilt” means that one mirror of the oscillator is tilted so that its axis is misaligned with the axis of the electron beam and undulator. A small amount of mirror tilt will greatly affect the FEL when compared to the effects of electron beam tilt. A mirror tilt on the order of magnitude of micro-radians will cause the extraction of the FEL to fall below the desired

levels. The reason for this is the same as for a mirror shift where the optical beam and the electron beam cannot fully interact. Figure 15 shows how the optical beam is not aligned with the electron beam due to the mirror tilt.

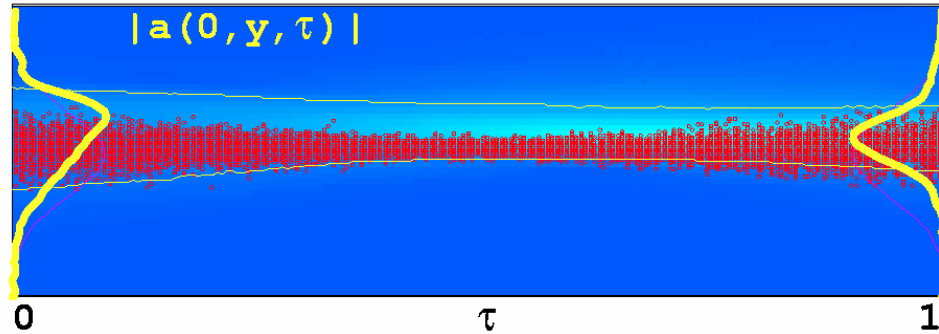


Figure 15. Optical energy in an oscillator FEL with a mirror tilt.

The capability to hold the mirrors in place with a precision of micrometers and microradians has already been shown in laboratories. While the ship vibrations are much larger than these tolerances (the largest required by MIL-STD-167-1A of 0.030 inches is about one ten times that of the FEL tolerance), isolation and active alignment should eliminate the problem. The methods of vibration mitigation will be examined in the following chapter.

THIS PAGE INTENTIONALLY LEFT BLANK

V. VIBRATION DAMPING

From the previous chapter we determined that the FEL cannot operate at full power if it is subject to mirror displacement or tilt greater than a few micrometers or microradians. In order to ensure that the ship vibrations do not cause the FEL to fail or to have fluctuating power, methods of mitigating the vibrations must be employed. Among the possible methods to reduce the effects of vibrations are to isolate the vibrations through a spring and damper system and to actively align the mirrors and the electron beam.

A. VIBRATION ISOLATION

The effect of the ship's vibrations can be lessened by using a system of springs and dampers placed between the ship and the FEL. In such a setup, key components of the FEL, such as the oscillator mirrors, undulator, electron beam path (and in an amplifier the seed laser) would be mounted to the ship with a spring-and-damper isolation system. This setup would not completely negate vibrations but would diminish their effect, especially in certain frequency bands.

A simple diagram of the isolation method which may be used is shown in Figure 16. In this case, a deck of the ship labeled S vibrates with the motion x_s . The mass m represents the portion of the FEL which is supported by the isolator. The spring constant is k and the amount of damping is characterized by c .

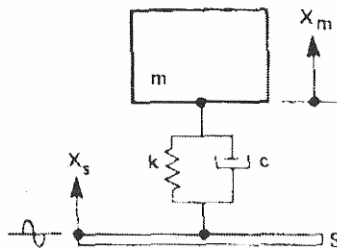


Figure 16. Diagram of a mass-spring-dashpot system with a vibrating support structure [From 13].

A spring-and-damper isolation system depends on viscous damping. In this case, the amount of transmissibility is shown in equation 5.1 [13]. Transmissibility T is the ratio of the FEL displacement to ship displacement, so a transmissibility of 0.1 would represent the FEL moving one-tenth the displacement of the ship. The transmissibility is $T=x_m/x_s$ where

$$T = \sqrt{\frac{1 + (2\zeta r)^2}{(1 - r^2)^2 + (2\zeta r)^2}} = \sqrt{\frac{1 + (\eta r)^2}{(1 - r^2)^2 + (\eta r)^2}}, \quad (5.1)$$

the damping ratio is $\zeta = c / c_{crit}$ where c is the damping coefficient of the damper and the critical damping coefficient is $c_{crit} = 2c_{char}$, where the characteristic resistance is $c_{char} = (km)^{1/2}$. The frequency ratio is $r = \omega / \omega_0$ where $\omega_0 = (k/m)^{1/2}$ is the resonant frequency. The value of the loss factor is $\eta = 1/Q = 2\zeta$ where the quality factor is $Q = c_{char}/c$. The effect of the frequency on the transmissibility is clear from equation 5.1. If the frequency is much below the critical frequency, meaning $r \ll 1$, then the transmissibility is $T \approx 1$. At larger frequencies where $r \gg 1$ the transmissibility will decrease, and go to zero as the frequency approaches infinity. At $r=1$, the transmissibility is at a maximum since this is driving on-resonance. The transmissibility as a function of the frequency ratio is shown in Figure 17.

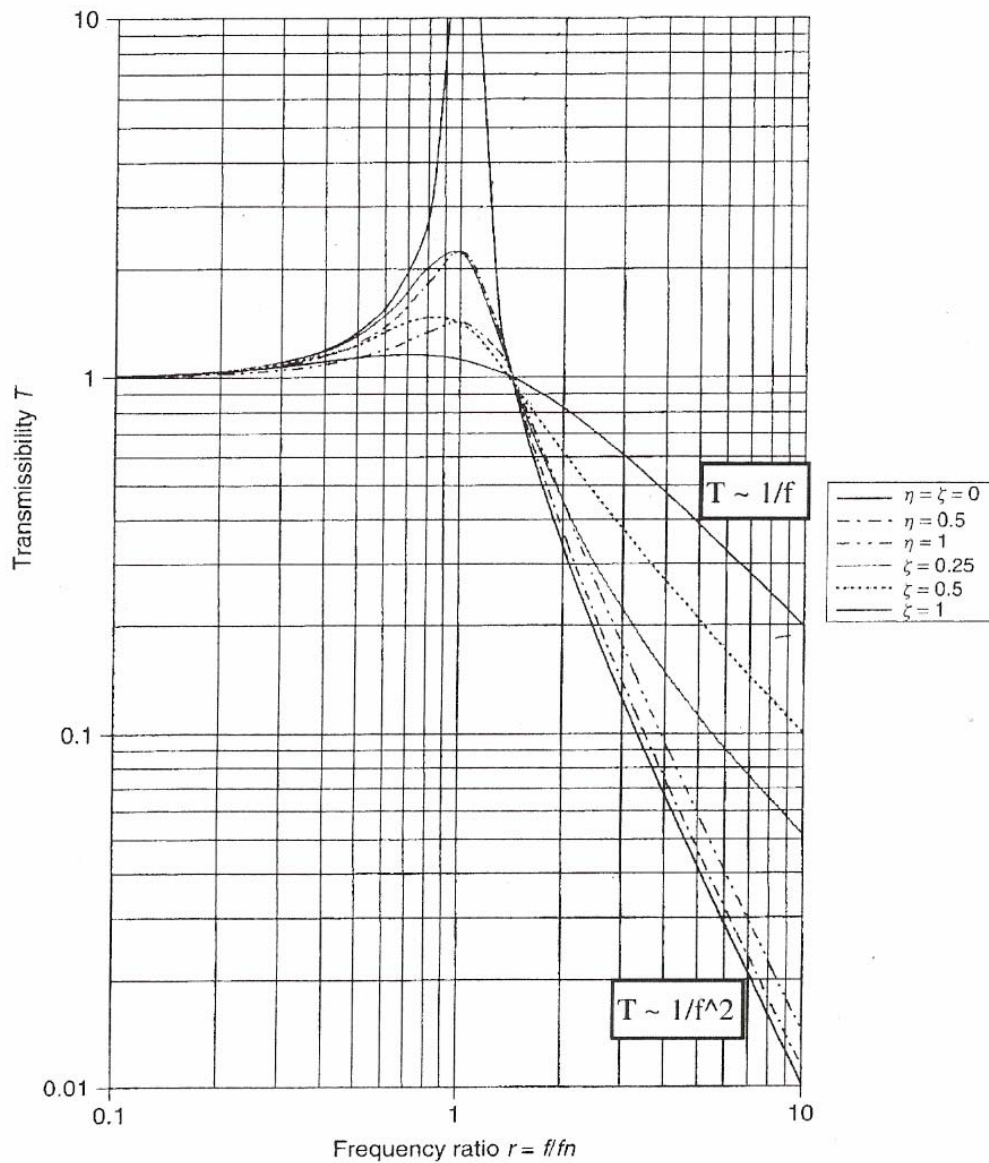


Figure 17. Transmissibility as a function of frequency ratio [From 13].

Since the transmissibility is one for the values of frequency where $r \ll 1$, the spring and damper system must be designed so that the resonant frequency is below the values expected for the system to undergo. The frequencies shown in table 2 of chapter four are all at low frequencies and the lowest have the highest amplitudes. The spring and damper system will therefore need to be designed so that the value of ω_0 is significantly less than 4Hz. This should not be difficult since the FEL components which

will be supported are rather massive and as long as the spring constant is not very large a spring and damper system will be suitable for the FEL.

B. ACTIVE ALIGNMENT

In order to prevent ship oscillations from having too large an effect, an active alignment system would be required. Such a system would consist of a group of low power lasers and a set of position sensitive devices. The system would use the lasers as a reference position and the position sensitive devices would measure the displacement from the reference. Then servos would reposition the mirrors and magnets would align the electron beam to the desired location.

Active alignment systems have been in use in laboratories and other applications for quite some time. One area in which active alignment and adaptive optics has especially been used is astronomy. Table 10 shows the tolerances required for a telescope called the Large Synoptic Survey Telescope (LSST) and gives tolerances of similar scale to those of the FEL within 5microns and 2arcseconds or about 10microradians [14]. Figure 18 also shows how the mirrors of the telescope are oriented.

Table 10. Tolerances for mirror and camera alignment of LSST.

Body Motion	Decenter	Tilts	Piston
M1, M3	Reference Optical Axis		
M2	+/- 10microns	+/- 5arcsec	+/- 10microns
Camera	+/-5microns	+/-2arcsec	+/-5microns

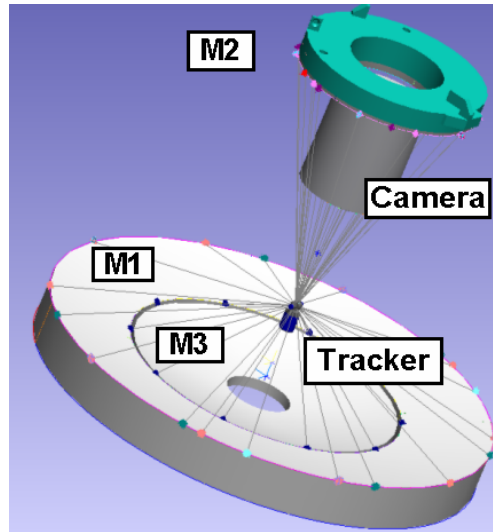


Figure 18. Diagram of mirror placement in LSST [From 14].

Besides its use in telescopes, active alignment is also used in laser systems. A good example of this is the Airborne Laser, in which the laser is designed to be carried on a modified Boeing 747. Since the platform is translating, twisting, and vibrating this laser has overcome similar problems as the FEL will face on board the all-electric ship. The active alignment system of the Airborne Laser was able to reduce the jitter on the internal resonator mirrors to less than $1\mu\text{rad}$ [15].

These examples show that the engineering challenges for similar systems have already been met. The effect of ship vibrations should therefore be lessened by both the vibration isolation methods as well as the active alignment system, so that the FEL will operate with the desired output power while on the all-electric ship.

THIS PAGE INTENTIONALLY LEFT BLANK

VI. WEIGHT, COST, AND SIZE

The FEL is, at present, a very large and heavy device. They are also expensive to build and to design. But, any other laser weapon of comparable power will be of similar size and cost. This chapter will examine the space, weight and cost of a shipboard FEL.

A. FEL WEIGHT AND SIZE

The weight of the FEL is of concern since it will be onboard a naval vessel, and may affect the behavior of the ship, depending on where it is placed. Table 11 below shows an estimate of the weight distribution of an FEL, as well as a comparison between the one-megawatt and three-megawatt FEL designs. The values in Table 13 are for oscillator FEL designs, but amplifier FELs have similar weights since the absence of mirrors somewhat offsets the heavier wigglers. The FEL component weights are found using the computer simulation program FELSIM from AES.

Table 11. Weight of FEL components of one and three-megawatt designs.

	1 MW	3 MW
Subsystem	Weight (kg)	Weight (kg)
Photocathode laser	450	700
DC Injector	2,950	4,450
LINAC	3,770	3,770
Wiggler	830	830
Beam stop	1,330	2,300
Cryoplant	12,650	10,220
RF power	8,100	20,430
RF distribution	5,380	13,380
HVDC(IGBT)	4,000	12,000
Matching sections	27,750	27,780
Totals	67,210	95,860

As can be seen in Table 11, the increase in power does lead to a weight increase, largely due to the increased power required for the three-megawatt design. That requires

more RF power and also a larger injector. Note that the one-megawatt design requires a larger cryoplant; this is because it is designed to operate continuously, whereas the three-megawatt design will have 300 shots worth of liquid helium stored, with the ability to replace this at a rate of 30 shots per hour.

The all-electric ship would have a displacement of about that of an aircraft carrier, 97,000 tons, of which the FEL would constitute less than 0.1%. For comparison, a current ship, the DDG-51 class, has a displacement of 8,300 tons and it has four General Electric LM2500 gas turbine engines each weighing 10,300 lbs [16]. This means that the weight of the engines is about 20.6 tons, about 0.25% of the total ship's weight. As the total FEL weight, 75-105 tons, is about sixteen times the weight of a single gas turbine engine, it is suited only to a large vessel, such as the all-electric ship.

The FEL is also large, occupying a box of about 20m long, by about 2.5m wide, and about 2.5m in height. This yields a total volume of about 130m^3 , which will compete with other ship systems. These dimensions are constrained by two components of the FEL: the SLINAC and the optical cavity in an oscillator FEL. They must each be about 20m long and cannot be made shorter.

These dimensions are much smaller than those of current FELs, which nevertheless have a maximum power of only about one percent of that of the FEL weapons system. (For example the FEL at Jefferson Lab is about 60m long and about 10m wide.) The reason for this is that current laboratories' FELs are designed so that they can be readily altered for experimentation and ease of access for mounting sensors and other diagnostic equipment. Thus a functional FEL on a ship will be much more compact. Surprisingly, the FEL takes up about the same amount of space regardless of the output power. This can be seen in Figure 19 where the size is a flat line at 130m^3 .

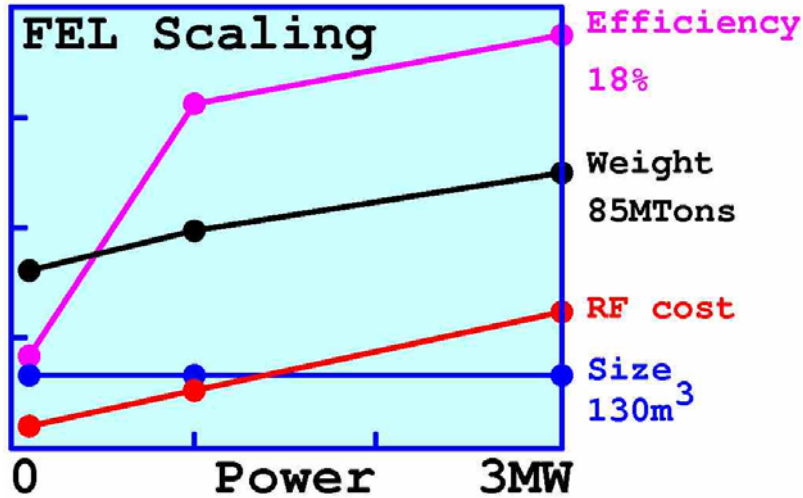


Figure 19. Graph of the cost, efficiency, weight, RF cost and size of 100kW, 1MW and 3MW FEL designs [From 7].

B. FEL COST

The FEL will be costly, but its price is similar to other weapons systems. The cost of the FEL will be on the order of about \$100million. This is comparable to the projected cost of other types of lasers.

To fire a single RIM-116 rolling airframe missile costs about \$440,000, so the FEL would cost much less to operate. In fact it would require only a small amount of fuel for each shot, about three gallons if electrical power is generated through a gas turbine. The FEL also will have a huge magazine capacity since each shot requires an insignificant amount of diesel fuel. Also, not having dangerous explosives on board could well save the occasional losses associated with an accidental explosion. These benefits along with the FEL's advantages of being a speed of light weapon help to justify the large initial cost.

THIS PAGE INTENTIONALLY LEFT BLANK

VII. CONCLUSION

The simulations of the FEL, the results from AES FELSIM and the methods to reduce the effects of vibrations show that it is feasible to place the FEL on the all-electric ship. It has been shown that the all-electric ship will have much more than the required amount of electrical power for the FEL to operate. The results of simulations show that the FEL will be able to tolerate mirror displacements of only a few microns or microradians and that ship vibrations will greatly exceed these limits. Solutions to reduce the effect of vibrations rely on both vibration isolation and active alignment systems, and they work. The weight and size of the FEL were also described so that it could be compared to other ship's systems.

Future work could examine the active alignment system in greater detail. The active alignment system as described in this thesis is meant to show that the system is feasible, but does not demonstrate exactly how such a system would be setup on the FEL. Also, more research needs to be done on the beam transport from the FEL to the beam director. Further work could also examine taking measurements of actual ship vibrations and running additional simulations to determine what the FEL output may be at different displacements.

THIS PAGE INTENTIONALLY LEFT BLANK

LIST OF REFERENCES

- [1] O'Shea, Patrick G. "Introduction to Free-Electron Lasers." 20 October 2003. DEPS Free Electron Laser Short Course. Albuquerque, NM. 25-26.
- [2] Brau, C. A. Free Electron Lasers. 1st Edition. Academic Press Inc. 1990.
- [3] Hughes, Michael. "SRF Gun Modeling." E-mail to author. 8 February 2007.
- [4] Centre Laser Infrarouge d'Orsay. "What is a Free-Electron Laser." April 2007.
- [5] Jackson, John David. Classical Electrodynamics. 3rd Edition. John Wiley & Sons Inc. 1999. 586.
- [6] Colson, W. B. Naval Postgraduate School,
a. PH4858 Class Lecture. NPS. Fall 2006.
b. and Pellegrini C., and Renieri A. Classical Free Electron Laser Theory. Chapter 5 in "Free Electron Laser Handbook." Elsevier Science Publishing Co. Inc. December 1990. 3-4.
c. "Efficiency." E-mail to author. 4 May 2007.
- [7] Advanced Energy Systems. Results from FELSIM Simulations of High Power FELs. January-February 2007.
- [8] Caryotakis, George. SLAC Klystron Lecture 1. Stanford University. 14 January 2004. [[http://www-group.slac.stanford.edu/kly/Lecture_Series/Klystron Lecture 1 slide show.ppt](http://www-group.slac.stanford.edu/kly/Lecture_Series/Klystron_Lecture_1_slide_show.ppt)], April 2007.
- [9] Wolff, Christian. 2007. "Klystron Amplifier." April 2007. [<http://www.radartutorial.eu/08.transmitters/tx12.en.html>].
- [10] Thales. "Thales Electron Devices." April 2007. [<http://www.capp.iit.edu/workshops/epem/Transparencies/Guidee.pdf>]. 7.
- [11] Integrated Publishing. "Electrical Engineering Training Series." [<http://www.tpub.com/neets/book11/45c.htm>], April 2007.
- [12] Zolfghari, A., MacGibbon, P., and North B. "Comparison of Klystron and Inductive Output Tubes (IOT) Vacuum-Electron Devices for RF Amplifier Service in Free-Electron Laser." Proceedings of EPAC 2004. [<http://filburt.lns.mit.edu/accelphy/Pubs/2004/TUPKF065.pdf>], April 2007.
- [13] Baker, Steven. Naval Postgraduate School. Lecture Notes January 2007.

[14] Gressler, William J. and Sandwith Scott. Active Alignment System for LSST. [http://www.kinematics.com/library/Active%20Alignment%20LSST_2006.ppt], May 2007.

[15] Morris, Dave. “Local Jitter Issues & Mitigation.” 14 July 2004. ABL Jitter Mitigation. 23 February 2007.

[16] GE Aviation Model LM2500. 2007. General Electric. [<http://www.geae.com/engines/marine/lm2500.html>], April 2007.

INITIAL DISTRIBUTION LIST

1. Defense Technical Information Center
Ft. Belvoir, Virginia
2. Dudley Knox Library
Naval Postgraduate School
Monterey, California
3. William B. Colson
Naval Postgraduate School
Monterey, California
4. Robert L. Armstead
Naval Postgraduate School
Monterey, California